ARTICLE IN PRESS

Quaternary International xxx (xxxx) xxx

Contents lists available at ScienceDirect

Quaternary International

journal homepage: www.elsevier.com/locate/quaint

Late Quaternary evolution of the Metaponto coastal plain, southern Italy, inferred from geomorphological and borehole data

Giuseppe Corrado [a], Giuseppe Aiello [b], Diana Barra [b,c], Paola Di Leo [a,d], Dario Gioia [e,*], Minervino Amodio Antonio [e], Roberta Parisi [b], Marcello Schiattarella [a]

[a] Dipartimento delle Culture Europee e del Mediterraneo (DiCEM), Basilicata University, I-75100, Matera, Italy
[b] Dipartimento di Scienze della Terra, dell'Ambiente e delle Risorse, Federico II University of Naples, Naples, Italy
[c] Istituto Nazionale di Geofisica e Vulcanologia, Sezione di Napoli, Osservatorio Vesuviano, Via Diocleziano 328, 80124, Naples, Italy
[d] CNR-IMAA, Tito Scalo, I-85050, Potenza, Italy
[e] CNR-ISPC, Tito Scalo, I-85050, Potenza, Italy

ARTICLE INFO

Keywords:
Coastal evolution
Paleoecology
Chronostratigraphy
Relative sea-level changes
Tectonic uplift
Southern Italy

ABSTRACT

A multidisciplinary study of a sector of the Ionian coastal belt, southern Italy, mainly based on two new boreholes approximately 25 m (MSA) and 20 m (MSB) deep, was carried out in the frame of a wider geo-archaeological project. Stratigraphic and Paleoecological data, together with geomorphological observations, have been used in order to define the Late Quaternary morpho-sedimentary evolution and its relationships with tectonic and climate forcing. The analyses of core sediments and geomorphic interpretations allowed us to reconstruct the changes in depositional setting and physical landscape starting from the MIS 5.5. To this scope, new data about sedimentary facies, benthic foraminifera and ostracod assemblages, and a set of ^{14}C ages spanning from about 33 to 15 kyr BP are here presented. All these data revealed a strong modification of the depositional setting within the coastal plain, as inferred by the presence of marine, transitional, and continental deposits, and suggest an anomalous position of sea-level reference points. Such anomalies are clustered in two homogenous arrays that can be explained only admitting a significant tectonic uplift in recent times (i.e. about 4 mm/yr over the last 15,000 years).

1. Introduction

The Metaponto coastal plain represents the most recent exposed sector of the southern Apennine foredeep (the so-called Bradano Trough, e.g. Migliorini, 1937; Pescatore et al., 2009, Fig. 1), a foreland basin that, at least since middle Pleistocene times, experiments a moderate and generalized tectonic uplift (Ciaranfi et al., 1983; Doglioni et al., 1994, 1996).

The need to better define the Quaternary and future evolution of the coastal areas is pushing on the scientific community to carry out new studies on coastal plains devoted to the reconstruction of ancient environmental scenarios in response to sea-level changes induced by climate and tectonic forcing. Such investigations require an interdisciplinary approach, which can benefit from an integration between traditional geological and geomorphological surveys and innovative methods such as geophysical imaging or remote sensing data (Wöppelmann and Marcos, 2016; Aucelli et al., 2012; Schaeffer et al., 2012; Antonioli et al., 2017; Di Paola et al., 2018; Amato et al., 2020; Di Lorenzo et al., 2021). Nowadays, one of the more consolidated approaches in studying the recent evolution of coastal plains includes the analysis of stratigraphic, sedimentological, radiometric, paleontological, and palynological features (Abate et al., 1998; Aiello et al., 2007, 2021; Aiello et al., 2021a,b; Barra et al., 1996, 1998; Cilumbriello et al., 2010; Marturano et al., 2011; Corrado et al., 2018, 2020). Such studies aim to illustrate the morpho-sedimentary evolution of the plains and/or to understand the forcing factors potentially responsible for coastal flooding and erosion. In fact, the coupling effect of sea-level rise and negative ground motions can be a determining factor in coastal vulnerability increase. In addition, low-lying coastal belts of active orogenic chains are sensitive areas in terms of climate-tectonics interplay.

In this work we have adopted a multidisciplinary approach to define the stratigraphic pattern and evolution of the Metaponto alluvial-coastal plain, located in Basilicata region (southern Italy), that can be useful for a comparison with sequences of morpho-evolutionary stages of other

* Corresponding author.
E-mail address: dario.gioia@cnr.it (D. Gioia).

Please cite this article as: Giuseppe Corrado, *Quaternary International*, https://doi.org/10.1016/j.quaint.2022.01.008

coastal plains of the Italian peninsula in the same geodynamic context (i.e., from the north, Sibari Plain, Rossano Plain, Messina Strait, Eastern Sicily). Many analyses have been performed on samples from two new cores drilled in the northern portion of the study area. The drilling survey and the location of the boreholes have been planned on the basis of the geomorphological study of the coastal strip, particularly in the part of the coastal plain. The geomorphological setting and the sedimentological and environmental features of the Metaponto Plain have been previously investigated by Cilumbriello et al. (2010) and Tropeano et al. (2013). Anyway, there are still some open issues on the evolution of this plain during the last 130 kyr. Our efforts aim to reconstruct in detail the Late Quaternary environmental conditions of the study area. To this scope, we present new data useful for a better definition of the morphotectonic, sedimentary, and sea-level changes that influenced the evolution of the plain during the upper part of the Pleistocene (starting from the Tyrrhenian stage) and the Holocene, through sedimentological,

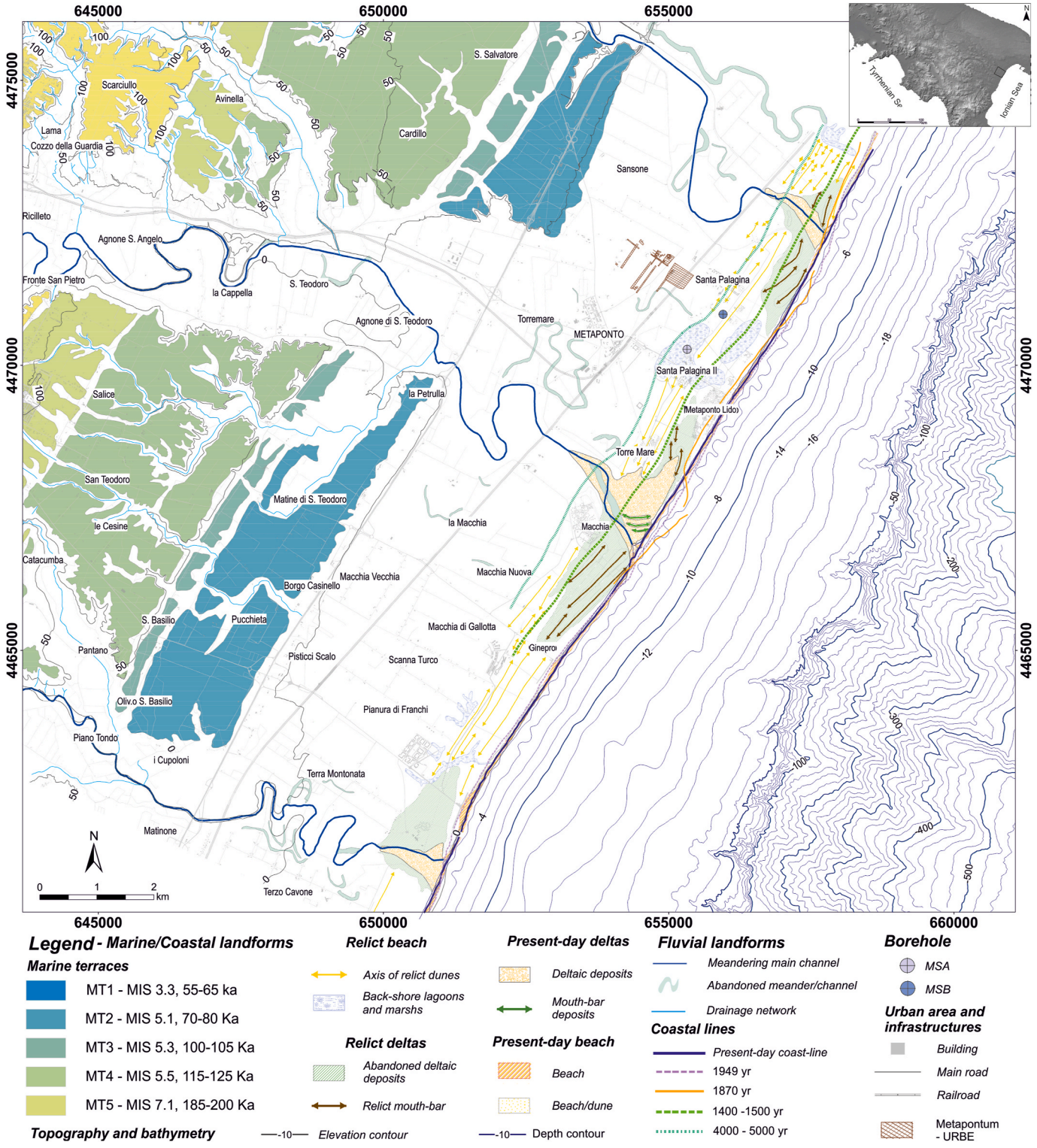

Fig. 1. Simplified geomorphological map of the study area.

paleoecological and radiometric analyses of a significant number of samples (i.e. about 70) from the two cores, enforcing the viability of a good correlation between them and the alternative interpretation of some key-features of the study area such as marine terraces and Paleocoastlines.

2. Regional setting

The study area is a large coastal plain located along the Ionian coastal belt of the Basilicata region, southern Italy. From a geological viewpoint, it coincides with the southernmost and youngest outcropping sector of the Bradano Foredeep, which underwent a progressive stage of emersion since the Middle Pleistocene (Corrado et al., 2017) because of the interplay between a moderate tectonic uplift (<1 mm/yr, Cucci and Cinti, 1998; Westaway, 1993; Schiattarella et al., 2006; Westaway and Bridgland, 2007) and eustatic sea-level cycles (Pescatore et al., 2009). A staircase of marine terraces ranging in altitude from 380 m a.s.l. to about 10–15 m a.s.l. is the main geomorphological evidence of such an evolution of the study area, and spatial and vertical distribution of marine terrace staircase has been extensively investigated to infer the tectonic evolution of this sector of southern Italy (Belluomini et al., 2002; Brückner, 1980; Caputo et al., 2010; Cilumbriello et al., 2010; De Santis et al., 2018; Gioia et al., 2016, 2018, 2020; Sauer et al., 2010; Zander et al., 2006), with controversial and debated results. Recent revision of the spatial distribution and chronological attribution of the several orders of marine terrace remnants allowed us to reconstruct 11 order of terraces ranging in age from about 600,000 to 60,000 yr (Gioia et al., 2018, 2020). Middle to Upper Pleistocene marine terraced deposits consist of thin gravel and sand wedges, which unconformably overlie Lower Pleistocene marine silty clays (Tropeano et al., 2002). The top of the Metaponto plain reaches a maximum elevation of ca. 15 m a.s.l. and leans landwards on the younger, Upper Pleistocene marine terrace of the study area. Morpho-sedimentary evolution of the Metaponto plain is the result of the complex sedimentary processes induced by progressive and discontinuous sea-level rise occurring after the fast base-level fall and related incision processes of the Last Glacial Maximum. The LGM Paleomorphology was buried below a ca. 100 m thick Upper Pleistocene - Holocene marine and continental sedimentary succession with a complex internal architecture (Cilumbriello et al., 2010; Grippa et al., 2011; Tropeano et al., 2013). The youngest deposits of the study area are related to the recent sedimentary processes occurring along the main meander-type rivers of the study area and to the delta and beach depositional systems. The present-day shore is featured by a low-gradient sandy beach that is limited landward by several meters-thick dunes, striking mainly parallel to the shoreline. Fine marshy deposits accumulated between these different generations of dunes (Fig. 1).

Until the land reclamation of the last century, the backshore area of the Metaponto coastal plain was characterized by wide limno-palustrine environments. The plain is now featured by sandy and silty meandering fluvial systems, with several artificial channels. Low-altitude areas of the coastal plain are still affected by occasional flooding events along the courses of the main streams during extreme rainfall (Pescatore et al., 2009).

3. Materials and methods

Two 20 m- and 25 m-deep cores were drilled in the northern portion of the Metaponto Plain (Fig. 1). The southernmost borehole MSA is located at 3 m a.s.l. in the municipality of Bernalda, at coordinates 16°49′46″ E, 40°22′6″ N (WGS84 coordinate system), near the Basento River mouth. The borehole MSB is also located at 3 m a.s.l. in the same municipality, at coordinates 16°50′13″ E, 40°22′26″ N (WGS84 coordinate system). Both are placed in back-dune areas, more than 1 km from the current coastline.

The cores were analysed to define texture, grain-size composition, fossil content, and sedimentary structure. The most significant layers were sampled for laboratory analyses, such as Paleoecology (based in particular on the analysis of ostracod and foraminiferal assemblages), and ^{14}C AMS dating. These analyses provided a basic contribution in interpreting the lithofacies associations, their chronology, and the original depositional environments.

The stratigraphic position of the horizons and samples from the two cores is referred exclusively to the elevation above sea level (a.s.l.). In the tables, on the contrary, also the depth value from the topographic surface is reported.

3.1. Paleoecological analysis

Paleoecological analyses have been performed on a total of 41 samples, 22 collected from the MSA core (Fig. 2) and 19 from the MSB core (Fig. 3).

Sediment samples were prepared according to the standard methods used for both ecological (e.g. Sgarrella and Barra, 1985; Aiello et al., 2021a,b) and paleoecological (e.g. Aiello et al., 2015; Aiello et al., 2018) investigations on benthic foraminiferal and ostracod assemblages. The collected samples were oven-dried at ~60 °C and scrubbed free of external contamination. They were then fragmented by hand until no fragment was larger than 1 cm^3. An amount of 100 g was weighted out of the samples and boiled with sodium carbonate solution for 20 min. The disaggregated samples were washed and sieved through two screens, the upper one having a mesh diameter of 125 μm (= 120 mesh) and the lower one a mesh diameter of 63 μm (230 mesh). The residues upon the screens were afterwards dried, split into aliquots with a dry microsplitter to yield about 300 benthic foraminiferal specimens (generally more abundant than ostracods), needed to assure statistical significance (Patterson and Fishbein, 1989), and examined under a reflected light binocular microscope. When fossil abundance was great a minimum of 300 specimens was picked per sample. In poor samples the entire content of benthic foraminiferal tests and ostracod shells was picked from the coarsest fraction (>125 μm), whereas, in rich ones only a suitable split was analysed. All the specimens were transferred to a microfaunal slide, sorted into species, identified, listed and counted for quantitative analysis.

Bivalves, bryozoans and gastropods (mostly fragments), charophyte oogonia, echinoderm spines, planktonic foraminifers, radiolarians and sponge spicules occurrences are reported as semiquantitative data (Tables 1 and 2).

Quantitative analysis has been conducted using number of foraminiferal specimens, ostracod Minimum Number of Individuals (MNI) and ostracod Total Number of Valves (TNV), normalized to 100 g of sediment sample (Tables 1 and 2). MNI has been calculated by adding the greater number between right and left adult valves to the number of adult carapaces; when only juveniles occur the MNI equals one. TNV includes all the juvenile and adult valves. Benthic foraminiferal and ostracod abundances (Individuals) and simple diversity (Taxa) are reported in Table 3. Benthic foraminiferal and ostracod taxa have been identified according to classic and modern literature both for benthic foraminifers and for ostracods (Aiello et al., 2018; Aiello et al., 2020; Aiello and Barra, 2010; Meisch, 2000 and references therein).

Two-way cluster analysis has been used to recognize groups of samples with similar taxonomic compositions (Q-mode) and groups of species that tend to co-occur (R-mode). Cluster analysis has been carried out for foraminiferal number of individuals (I) and minimal number of ostracod individuals (MNI) and, separately, for foraminiferal specimens and the total number of ostracod valves (TNV) to compare results obtained with different methods to count ostracod specimens. Similarity has been determined using a paired group algorithm and the Morisita similarity index. Benthic foraminiferal and ostracod species with relative species abundance RSA >5% in at least one sample have been taken into account.

Statistical analysis has been performed with PAST software (Hammer

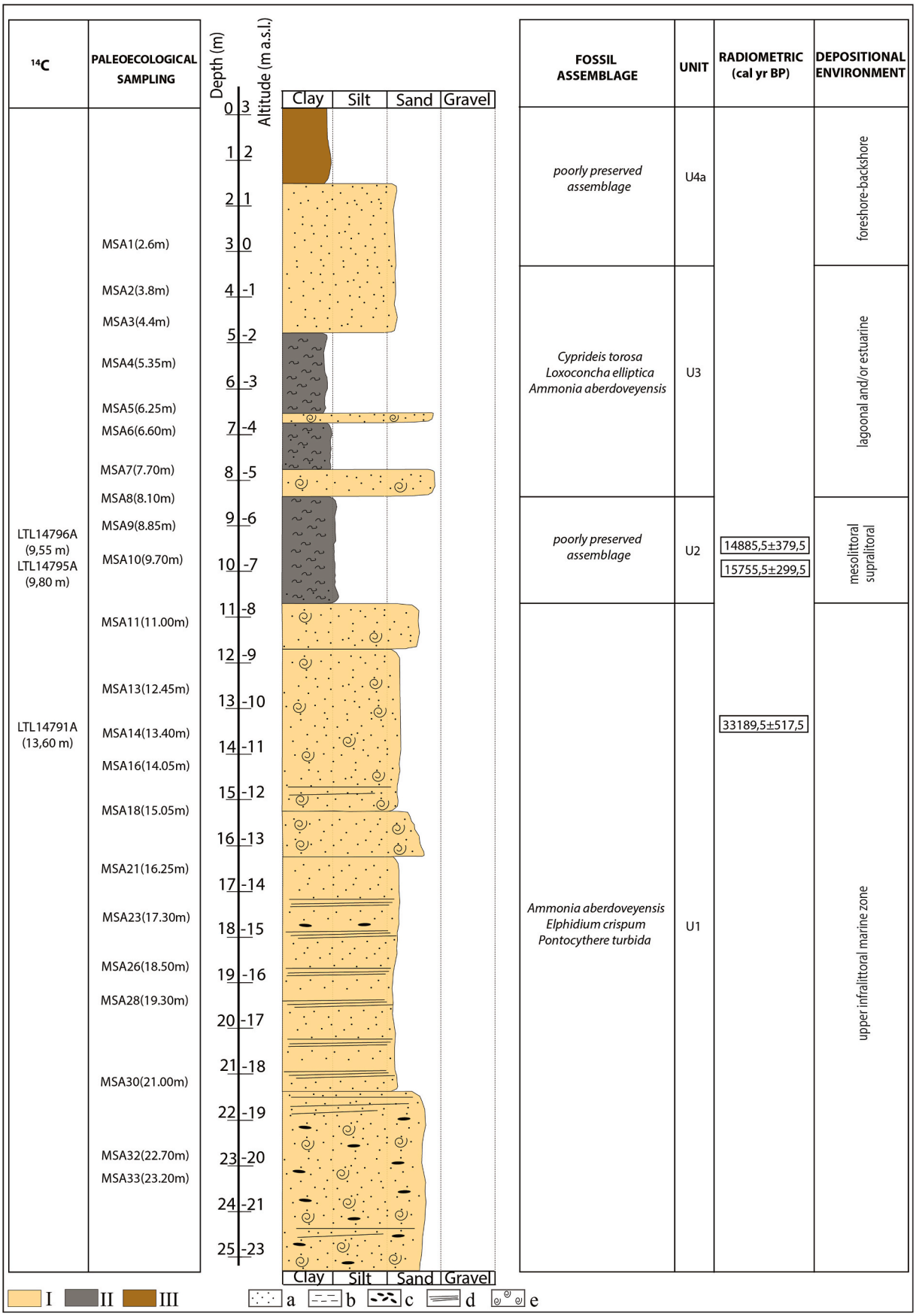

Fig. 2. Simplified Sedimentological log of the core MSA. (I) marine sand, (II) transitional deposits, (III) continental and anthropic deposits, (a) sands, (b) clay, (c) pebbles, (d) lamination, (e) fossil.

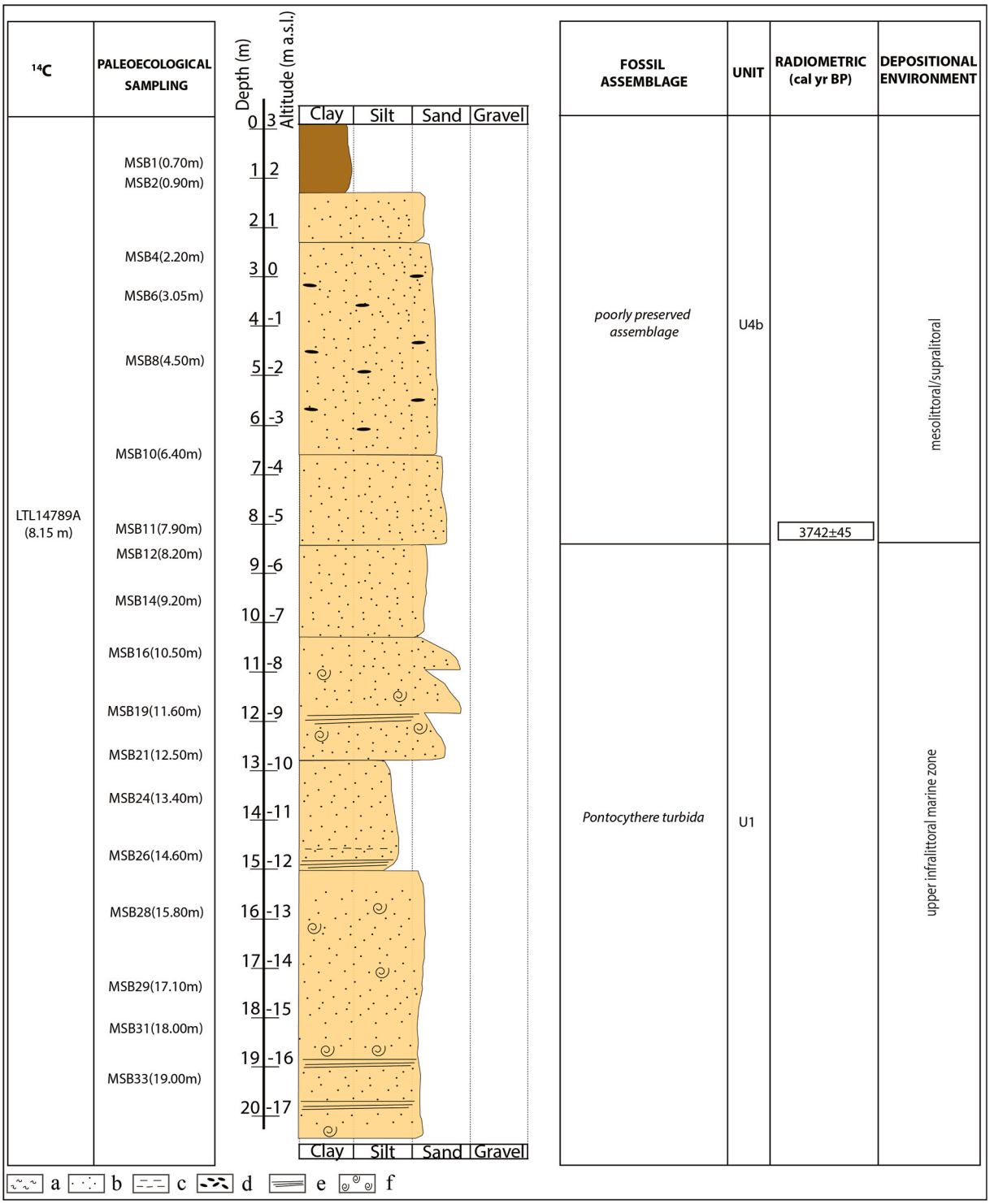

Fig. 3. Simplified Sedimentological log of the core MSB. (I) marine sand, (II) transitional deposits, (III) continental and anthropic deposits, (a) sands, (b) clay, (c) pebbles, (d) lamination, (e) fossil.

et al., 2001)

Since the majority of the fossil assemblages consist of ecologically incompatible species (e.g. co-occurrence of marine planktic, marine benthic circalittoral, brackish and freshwater benthic taxa), they have been generally considered mixed assemblages (*sensu* Fagerstrom, 1964). The observation of the state of preservation, together with the co-occurrence of young and adult stages, has been highly effective in discriminating between allochthonous and autochthonous ostracod shells. Due to the delicate structure of the valves, they are very sensitive to transport processes. On the other hand, the auto-allochthoneity of foraminiferal tests, which frequently show high strength and toughness (*sensu* Aiello et al., 2006; Aiello et al., 2012; Aiello et al., 2020; Zuschin et al., 2003) could not be undoubtedly determined, at least in some cases. Consequently, despite the benthic foraminiferal abundances are generally higher than those of ostracods, paleoecological reconstructions have been performed taking into account primarily the ostracod signal, using the foraminiferal data to support the interpretation.

Table 1
Semiquantitative distribution of microfossils remains (VR = very rare; R = rare; U = uncommon; C = common), benthic foraminiferal absolute abundance (I = individuals per 100 g of sediment), ostracod absolute abundance [I(MNI) = minimum number of individuals per 100 g of sediment; j indicates juvenile specimens] and ostracod absolute abundance [I(TNV) = total number of valves) per 100 g of sediment] from core MSA.

samples	MSA 33	MSA 32	MSA 30	MSA 28	MSA 26	MSA 23	MSA 21	MSA 18	MSA 16	MSA 14	MSA 13	MSA 11	MSA 10	MSA 9	MSA 8	MSA 7	MSA 6	MSA 5	MSA 4	MSA 3	MSA 2	MSA 1
meters	23.20	22.70	21.00	19.30	18.50	17.30	16.25	15.05	14.05	13.40	12.45	11.00	9.70	8.85	8.10	7.70	6.60	6.25	5.35	4.44	3.80	2.60
Bivalvia	VR	R	VR	R	VR	VR	VR	R	C	VR	R		R			U	R	R	VR			
Bryozoa			VR																			
Characeae			VR					VR						VR								
Echinodermata	R		R	R	VR	R	VR	R	R	R	VR	U	VR			R	R	R				
Foraminifera (planktonic)	C	U	C	C	U		U	C	C	C	U	C	VR	R		R	VR	VR	VR			VR
Gastropoda	VR	R	VR		VR	VR	VR		C	VR	R	R		U	R	U		U	VR	VR	U	U
Porifera	U	R	U	R	R	R	R	U	C	C	R	C				VR		R				VR
Radiolaria																VR	R					
Foraminifera																						
Adelosina elegans (Williamson, 1858)		16																				
Adelosina longirostra (d'Orbigny, 1826)	192	48	224	88	20	28	128	24	16	8	4											
Adelosina mediterranensis (Le Calvez and Le Calvez, 1958)		16																				
Adelosina sp.				8		4																
Ammonia aberdoveyensis Haynes, 1973 lobate form			8														8	4	2		2	
Ammonia aberdoveyensis Haynes, 1973 rounded form	400	480	464	240	44	144	232	152	84	120	64	112	1	12	8	16	5	9		1		
Ammonia beccarii (Linnaeus, 1758)	72	128	56	24	16	28	64	48	16	16	24			12	6	12	3	3				
Amphicoryna scalaris (Batsch, 1791)				8				8	8													
Asterigerinata mamilla (Williamson, 1858)								8		4		4										
Astrononion stelligerum (d'Orbigny, 1839)						4						4										
Aubignyna perlucida (Heron-Allen and Earland, 1913)											4											
Bigenerina nodosaria d'Orbigny, 1826					2			8			4	4						1				
Bolivina alata (Seguenza, 1862)												4										
Bolivina catanensis Seguenza, 1862							24			4								1				
Brizalina spathulata (Williamson, 1858)	80	112	104	72	8	24	16	40	12	28	24	44						3				
Brizalina striatula (Cushman, 1922)				16			8	8	4		4											
Buccella granulata (Di Napoli Alliata, 1952)	88		72	48	4	40	16	24	8	4		32									1	2
Bulimina aculeata d'Orbigny, 1826	272	400	200	144	30	100	80	80	20	28	52	36										
Bulimina elongata d'Orbigny, 1846	24	96	32	40	10	20	8	16		12	24	4										
Bulimina striata d'Orbigny, 1832		16			2		16				4											
Cassidulina carinata Silvestri, 1896	648	768	632	528	82	228	352	560	164	384	316	356	1	8		2	2	19	1	1		
Cibicides lobatulus (Walker & Jacob, 1798)	136	32	160	104	10	76	8	96	72	64	44	64			2			3				
Cibicidoides bradyi (Trauth, 1918)												4										
Cibicidoides pachyderma (Rzehak, 1886)	256	176	232	208	26	184	192	400	92	108	88	164		4	4	16		6			1	
Cibicidoides robertsonianus (Brady, 1881)		32		8				8	8		4											
Cibicidoides variabilis (d'Orbigny, 1826)								8														
Cornuspira involvens (Reuss, 1850)							8					4										
Cycloforina contorta (d'Orbigny, 1846)			8				24															
Cycloforina villafranca (Le Calvez and Le Calvez, 1958)	8																					
Discorbinella bertheloti (d'Orbigny, 1839)	8	16					8	16				4										
Elphidium articulatum (d'Orbigny, 1839)				8	2		8							4								
Elphidium complanatum (d'Orbigny, 1839)	8	16					8			4	4											

(*continued on next page*)

Table 1 (*continued*)

samples	MSA 33	MSA 32	MSA 30	MSA 28	MSA 26	MSA 23	MSA 21	MSA 18	MSA 16	MSA 14	MSA 13	MSA 11	MSA 10	MSA 9	MSA 8	MSA 7	MSA 6	MSA 5	MSA 4	MSA 3	MSA 2	MSA 1
Elphidium crispum (Linnaeus, 1758)	120	336	152	88	18	76	112	104	72	56	20	56		4	2	18	9	8	1			
Elphidium granosum (d'Orbigny, 1826)	120	48	128	32	2	44	72	40	12	12	4	16						2				
Elphidium macellum (Fichtel & Moll, 1798)						4																
Elphidium poeyanum (d'Orbigny, 1839) DS form												4		8			2	1				
Elphidium poeyanum (d'Orbigny, 1839) FS form	24	32	72	16		20	8	24		28	4	4	1					1				
Elphidium pulvereum Todd, 1958					2																	
Elphidium punctatum (Terquem, 1878)			48	8		12	16	16	8	16	8	12										
Epistominella sp.											4											
Favulina hexagona (Williamson, 1848)																			1			
Fissurina orbignyana Seguenza, 1862								8														
Globobulimina affinis (d'Orbigny, 1839)	8	16		16				16	4		4	4						1				
Globocassidulina subglobosa (Brady, 1881)	48	16	32	24				32	16	16	12	8						1			1	
Gyroidinoides soldanii (d'Orbigny, 1826)	8	64	56	40		16		32	4	8	4							1				
Gyroidinoides umbonata (Silvestri, 1898)	8		8						4													
Haynesina germanica (Ehrenberg, 1840)														8				1				
Hoeglundina elegans (d'Orbigny, 1826)		16					8	8		8	16	12				2						
Hyalinea balthica (Schroeter, 1783)			40	48			8			16		4						1				
Laevidentalina sp.	24	16			4		8					4										
Lagena semistriata Williamson, 1848																				1		
Lenticulina inornata (d'Orbigny, 1846)	32	32				4	8	24	12	4	8							1				
Lenticulina orbicularis (d'Orbigny, 1826)		16							12													
Marginulinopsis costata (Batsch, 1791)							8															
Melonis affinis (Reuss, 1851)	104	144	112	56	12	16	72	56	44	36	28	32						1				
Neoconorbina terquemi (Rzehak, 1888)	8	32		8		4				8	4	12						2				
Nonion fabum (Fichtel & Moll, 1798)						4	8															
Oridorsalis umbonatus (Reuss, 1851)	8		8	16	2		8				8							2				
Planulina ariminensis d'Orbigny, 1826	48	32	56	48	10	40	48	64	24	28	8	16				2		1				
Pseudoclavulina crustata Cushman, 1936	16		8						12													
Pullenia bulloides (d'Orbigny, 1846)	16	32			12	8	16		16	12	8	4										
Pyrgo inornata (d'Orbigny, 1846)	8	16		8																		
Quinqueloculina lata Terquem, 1876	32	16							16			16	1									
Quinqueloculina padana Perconig, 1954	16		8	16	2			24				8					1					
Quinqueloculina pygmaea Reuss, 1850								16										1				
Quinqueloculina seminulum (Linnaeus, 1758)	64	64	48	24	6	12	8	24		4	8	4										
Quinqueloculina viennensis Le Calvez and Le Calvez, 1958	136	112	24	64	2	16	48	64	56	20	20					4		2				
Quinqueloculina sp.	8		8																			
Reussella spinulosa (Reuss, 1850)				8				8														
Rosalina floridana (Cushman, 1922)										4												
Sigmoilopsis schlumbergeri (Silvestri, 1904)					4			8			4			4								
Siphonaperta agglutinans (d'Orbigny, 1839)	24	48	24	16			24	8														
Siphonaperta aspera (d'Orbigny, 1826)	24		24			24		16		4								1				
Siphonaperta dilatata (Le Calvez and Le Calvez, 1958)	40	80	24	32	8	12	24	32	32	28	20	28		4		2						
Siphonina reticulata (Czjžek, 1848)	16		16					8									1					

(*continued on next page*)

Table 1 (*continued*)

samples	MSA 33	MSA 32	MSA 30	MSA 28	MSA 26	MSA 23	MSA 21	MSA 18	MSA 16	MSA 14	MSA 13	MSA 11	MSA 10	MSA 9	MSA 8	MSA 7	MSA 6	MSA 5	MSA 4	MSA 3	MSA 2	MSA 1
Siphonodosaria sp.		16		8		4	8			4	8	4										
Sphaeroidina bulloides d'Orbigny, 1826	8	224	8	8	12	8	56			4	4							4				
Spiroloculina depressa d'Orbigny, 1826											4											
Spiroplectinella wrightii (Silvestri, 1903)	24						8															
Textularia agglutinans d'Orbigny, 1839									4													
Textularia calva Lalicker, 1935	16	32	16					8		4												
Triloculina eburnea d'Orbigny, 1839			8																			
Triloculina oblonga (Montagu, 1803)	24				4	12	32															
Triloculina plicata Terquem, 1878		16																				
Triloculina schreibersiana d'Orbigny, 1839	32	64	88	32	14	16	40	24		8												
Triloculina trigonula (Lamarck, 1804)	136	128	112	56		44	56	24	8	8		4										
Uvigerina peregrina Cushman, 1923	584	736	368	176	50	148	256	176	108	52	40	20		4		4	1	2				
Uvigerina sp.											4											
Valvulineria complanata (d'Orbigny, 1846)	184	304	200	72	10	56	88	88	32	68	40	16		4		4		7			2	
species indeterminate	80	192	168	80		48	112	160	88	100	24	116				20						
Ostracoda MNI																						
Bosquetina sp.				8																		
Callistocythere flavidofusca (Ruggieri, 1950)								8														
Carinocythereis whitei (Baird, 1850)		16	8							4												
Cistacythereis turbida (G.W. Müller, 1894)							8															
Cyprideis torosa (Jones, 1850)					2		j							168 j		j	2 j	7 j	j	2 j	4 j	
Cypridopsis vidua (G.W. Müller, 1776)														12 j								
Cypris pubera O.F. Müller, 1776																		j				
Cytheretta subradiosa (Roemer, 1838)	16 j							16			4											
Cytheridea neapolitana Kollmann, 1960		16	8					8		4												
Cytheropteron latum G.W. Müller, 1894												4										
Echinocythereis sp.						4																
Henryhowella sarsi (G.W. Müller, 1894)	16		8	8																		
Heterocythereis voraginosa Athersuch, 1979										4												
Ilyocypris aff. *inermis* Kaufmann, 1900																		1	j			
Leptocythere macella Ruggieri, 1975																	1	1				
Loxoconcha elliptica Brady, 1868					2							4 j		4 j			3 j	2 j	j			
Loxoconcha ovulata (Costa, 1853)							8															
Loxoconcha sp.	8					4																
Palmoconcha turbida (G.W. Müller, 1894)		16																				
Pontocythere turbida (G.W. Müller, 1894)	32 j	16 j	32	16			32	16 j	4	4		8 j										
Pseudocandona sarsi (Hartwig, 1899)																		j				
Pseudolimnocythere hartmanni Danielopol, 1979																		1				
Semicytherura incongruens (G.W. Müller, 1894)			16		2		32	8														
Semicytherura sulcata (G.W. Müller, 1894)							8															
Urocythereis schultzi (Hartmann, 1958)								8														
Urocythereis sp.								8														
Ostracoda TNV																						

(*continued on next page*)

Table 1 (*continued*)

samples	MSA 33	MSA 32	MSA 30	MSA 28	MSA 26	MSA 23	MSA 21	MSA 18	MSA 16	MSA 14	MSA 13	MSA 11	MSA 10	MSA 9	MSA 8	MSA 7	MSA 6	MSA 5	MSA 4	MSA 3	MSA 2	MSA 1
Bosquetina sp.				8																		
Callistocythere flavidofusca (Ruggieri, 1950)								8														
Carinocythereis whitei (Baird, 1850)		32	8							4												
Cistacythereis turbida (G.W. Müller, 1894)							8															
Cyprideis torosa (Jones, 1850)					2		8							1780		4	7	47	1	60	313	
Cypridopsis vidua (G.W. Müller, 1776)														48								
Cypris pubera O.F. Müller, 1776																		2				
Cytheretta subradiosa (Roemer, 1838)	32							24			4											
Cytheridea neapolitana Kollmann, 1960		16	8					8		4												
Cytheropteron latum G.W. Müller, 1894												4										
Echinocythereis sp.						4																
Henryhowella sarsi (G.W. Müller, 1894)	16		8	8																		
Heterocythereis voraginosa Athersuch, 1979										4												
Ilyocypris aff. *inermis* Kaufmann, 1900																		1	2			
Leptocythere macella Ruggieri, 1975																	1	2				
Loxoconcha elliptica Brady, 1868					4							8		16			12	11	3			
Loxoconcha ovulata (Costa, 1853)							8															
Loxoconcha sp.	8					4																
Palmoconcha turbida (G.W. Müller, 1894)		16																				
Pontocythere turbida (G.W. Müller, 1894)	72	32	56	16			40	56	4	4		16										
Pseudocandona sarsi (Hartwig, 1899)																		1				
Pseudolimnocythere hartmanni Danielopol, 1979																		1				
Semicytherura incongruens (G.W. Müller, 1894)			24		2		40	8														
Semicytherura sulcata (G.W. Müller, 1894)							8															
Urocythereis schultzi (Hartmann, 1958)								8														
Urocythereis sp.								8														

All the studied specimens are housed in the Aiello Barra Micropaleontological Collection (A.B.M.C.) at the Dipartimento di Scienze della Terra, dell'Ambiente e delle Risorse, Università degli Studi di Napoli Federico II.

3.2. Radiometric, stratigraphic, and geomorphological analyses

An accurate stratigraphic description of the two cores, based on grain-size analysis, sedimentary structures, and fossils content, has been done: two stratigraphic logs have been so obtained (Figs. 2 and 3) and four stratigraphic units defined. Three samples from the MSA borehole and one sample from the MSB borehole have been chosen for radiocarbon dating procedure using high-resolution mass spectrometry technique (AMS) at the Dating and Diagnostics Center of the University of Salento (CEDAD). The selection of bulk sediment samples for radiocarbon dating has been done on the basis of the individuation of the following suitable stratigraphic layers:

- The LTL14796A sample (clay, 9.55 m from the top, −6.50 m a.s.l.; Fig. 2)
- The LTL14795A sample (clay, 9.80 m from the top, −7 m a.s.l.; Fig. 2)
- The LTL14791A sample (fine sands, 13.6 m from the top, −10.6 m a.s.l.; Fig. 2)
- The LTL14789A sample (fine-medium sands, 10 m from the top, −7 m a.s.l. Fig. 3).
- The LTL14789A sample (fine-medium sands, 10 m from the top, −7 m a.s.l.; Fig. 3).

The radiocarbon dating has been performed on the following clay and fine sand relatively rich in organic matter, and calibrated in calendar age using the OxCal 3.10 software based on atmospheric data (Reimer et al., 2016).

The geomorphological study has been mainly focused on the definition of the different generations of Late Quaternary marine terraces, based on both a detailed review of the literature describing these morphological features (Belluomini et al., 2002; Brückner, 1980; Caputo et al., 2010; Cilumbriello et al., 2010; De Santis et al., 2018; Gioia et al., 2020; Piccarreta et al., 2011; Sauer et al., 2010; Westaway and Bridgland, 2007; Zander et al., 2006) and original observations in the field and by aerial photos useful to re-interpret the meaning of some geomorphic markers.

4. Results

4.1. Stratigraphic and radiometric data

The study area consists of a flat portion (Santa Pelagina locality) of the coastal plain between the terraces staircase to the back and the dune-beach system. It is characterized by the presence of continental and transitional deposits: the first represented by fine-to coarse-grained sediments attributed to eluvial, fluvial, lacustrine, and palustrine environments, whereas the second ones are constituted of sands and silts of beach and deltaic environments (Fig. 1). Marine deposits are present at small depth in the subsurface (Figs. 2 and 3). The limit between the coastal plain and the Ionian Sea is represented by the present-day shore, which can be morphologically ascribed to the category of straight beach shoreline. The shore is a low-gradient sandy beach that is limited landward by several meters-thick sand dunes, striking mainly parallel to the shoreline. Fine marshy deposits accumulated between these different generations of dunes. In this coastal sector, the rivers show a meandering trend developing on relatively wide alluvial valleys which are embanked in the Pleistocene marine terraces and in the clay bedrock.

In this work, four major units (Figs. 2 and 3) have been identified within the succession of the Metaponto coastal plain reconstructed on the basis of core data. Such units, which constitute the Late Pleistocene – Holocene substrate of the plain, are reported in the followings:

- Unit 1 (U1) consists of fining-upwards medium-sized sand with pebbles and shell fragments
- Unit 2 (U2) is made up of greenish-grey clays with shell fragments
- Unit 3 (U3) is made up of sandy clay with interbedded cm-thick sandy levels
- Unit 4 is divided into units 4a (U4a) and 4b (U4b), the first being mainly made of fine sands whereas the second one is constituted of medium and fine sands with rare pebbles.

The radiometric dating of samples from MSA and MSB cores gave the following results:

- The LTL14796A sample (clay from MSA core, 9.55 m from the top, −6.50 m a.s.l.; Fig. 2) furnished a ^{14}C age of 14,885.5 ± 379.5 years BP;
- The LTL14795A sample (clay from MSA core, 9.80 m from the top, −7 m a.s.l.; Fig. 2) gave a ^{14}C age of 15,755.5 ± 299.5 years BP;
- The LTL14791A sample (fine sands from MSA, 13.6 m from the top, −10.6 m a.s.l.; Fig. 2) gave a ^{14}C age of 33,189.5 ± 517.5 years BP
- The LTL14789A sample (fine-medium sands from MSB core, 10 m from the top, −7 m a.s.l.; Fig. 3) provided a ^{14}C age of 3742 ± 45 years BP.

4.2. Paleoecology

Benthic foraminiferal assemblages include 106 species (13 in open nomenclature and one with affinitive status due to the poor state of preservation) in 61 genera.

Ostracod assemblages consist of 33 species (four left in open nomenclature and one with affinitive status due to the poor state of preservation) in 26 genera. A total of 6894 foraminiferal tests and 1046 ostracod valves have been studied. Species are listed in Appendix 1.

Benthic foraminiferal remains are present in all the samples of the MSA core. Ostracods are not recorded in the samples MSA 10, MSA 8 and MSA 1.

Benthic foraminiferal assemblages are dominated by the genera *Ammonia* (two species), *Elphidium* (eight species), *Cibicidoides* (four species), *Cassidulina* and *Uvigerina* (one species). Ostracod assemblages are characterized by *Pontocythere turbida* and *Cyprideis torosa*; *Loxoconcha elliptica* is relatively well represented and *Semicytherura incongruens* is an accessory species. Rare and scattered freshwater ostracod species pertaining to the genera *Cypris*, *Cypridopsis*, *Ilyocypris* and *Pseudocandona* have been recorded in the upper part of the section.

Benthic foraminifers are present in all the samples of the MSB core. The commonest species are *Ammonia aberdoveyensis*, *Cassidulina carinata*, *Cibicidoides pachyderma* and *Elphidium crispum*. Ostracod assemblages, characterized by *Pontocythere turbida*, occurred in eight samples of the core MSB, with low abundance values.

4.2.1. Cluster analysis

4.2.1.1. Core MSA. Three groups of samples have been identified through a two-way cluster analysis based on foraminiferal and ostracod Minimal Number of Individuals and Total Number of Valves abundances (Figs. 4 and 5). Only slight differences have been noted between MNI and TNV cluster analysis.

The sample MSA 1, displaying the lowermost faunal diversity of the section, has been individually discriminated; the rare fossil remains are here very poorly preserved.

The Cluster 1a (MNI) and the Cluster IIa (TNV) consist of, respectively, five (MSA 2-MSA 4, MSA 6, MSA 9) and six (MSA 2-MSA 6, MSA 9) samples, characterized by euryhaline, brackish and stress tolerant

taxa such as the ostracods *Cyprideis torosa* and *Loxoconcha elliptica* and the benthic foraminifers *Ammonia aberdoveyensis* (lobate form, LF) and *Elphidium poeyanum* (morph with depressed sutures, DS); the cluster Ba (MNI) and the cluster βa (TNV) include all the species and morphs typical of marginal brackish paleoenvironment.

The cluster 2a (MNI) and the cluster Ia (TNV) are formed by the remaining samples; the sample MSA 5 is included in the former cluster and excluded in the latter one. Their meiofunal assemblages consist mainly of marine stenohaline taxa typical both of upper infralittoral (e.g. *Ammonia aberdoveyensis*, *Pontocythere turbida*) and circalittoral-bathyal (e.g. *Cassidulina carinata*, *Henryhowella sarsi*) zone, grouped in both the cluster Aa (MNI) and αa (TNV). They are ecologically incompatible, and their co-occurrence indicates the presence of remarkable transport processes during the deposition of the succession.

4.2.1.2. Core MSB. The two-way cluster analysis performed on foraminiferal abundance and ostracod Minimal Number of Individuals and Total Number of Valves abundances (Figs. 6 and 7) individuate two clusters and a single sample (MSB 6). Clusters 1b (MNI) and Ib (TNV) include marine benthic foraminiferal and marine ostracod assemblages. Benthic foraminifers are represented by both upper infralittoral and circalittoral/bathyal species, whereas all the ostracods pertain to species typical of infralittoral waters, except the circalittoral/bathyal species *Bosquentina rhodiensis*, occurring in the sample MSB 16 in a very poor state of preservation. Clusters 2b (MNI) and IIb (TNV), as well as the sample MSB 6, include assemblages devoid of ostracod shells.

4.2.2. Meiofaunal associations

4.2.2.1. Core MSA. Q-mode cluster analysis of meiofaunal abundances of the Core MSA produced, both with the Minimum Number of ostracod Individuals (MNI) and with the Total Number of ostracod Valves (TNV), two recognizable sample clusters, defined by combinations of taxa from two discrete clusters recognized in the R-mode analysis. Four associations (indicating different biofacies) can be described: a high energy, low abundance/diversity, marine infralittoral association, dominated by benthic foraminiferal marine taxa and devoid of ostracod species; a benthic foraminiferal high abundance/diversity, marine infralittoral association, including the infralittoral marine ostracod species *P. turbida*; a brackish meiofaunal low-abundance association and a brackish association characterized by *C. torosa*. The most important species have been figured in Fig. 8; their ecological distribution data have been reported in Meisch (2000); Aiello et al. (2018), 2020, 2021, and literature therein.

4.2.2.2. High energy infralittoral marine association. This association is defined by Q-mode clusters 1a (MNI) – IIa (TNV) and by R-mode clusters Aa (MNI) – αa (TNV). It is characterized by *Elphidium crispum*, by the rounded morph of *Ammonia aberdoveyensis* and by A. beccarii, showing a very shallow marine depositional environment. Ostracods are not present, whereas reworked specimens of circalittoral-bathyal foraminiferal species, such as *C. carinata*, *C. pachyderma*, *Uvigerina peregrina* and *Valvulineria complanata*, are not rare. The association is representative of a high energy infralittoral marine paleoenvironment, where only foraminiferal species possessing a robust test could be preserved.

4.2.2.3. Infralittoral marine association. The association, which is defined by Q-mode clusters 2a (MNI) – Ia (TNV) and by R-mode clusters Aa (MNI) – αa (TNV), consists of abundant and differentiated shallow marine taxa. Characteristic autochthonous species are *Adelosina longirostra*, A. *aberdoveyensis* (rounded form), A. *beccarii*, *Buccella granulata*, *Bulimina aculeata*, *Cibicides lobatulus*, *E. crispum*, *Elphidium poeyanum* (morph with flush sutures) and the ostracod species *P. turbida*, all indicative of infralittoral marine waters. The allochthonous circalittoral-bathyal taxa are common and abundant.

4.2.2.4. Brackish water association. This association, defined by Q-mode clusters 2a (MNI) – Ia (TNV) and by R-mode clusters Ba (MNI) – βa (TNV), is characterized by the occurrence, with low abundance values, of the brackish ostracod species C. *torosa* and *Loxoconcha elliptica*, and the presence of two morphs of benthic foraminiferal species typical of marginal environments, i.e. *A. aberdoveyensis* (lobate form) and *E. poeyanum* (with depressed sutures).

4.2.2.5. Cyprideis torosa association. The association is defined by Q-mode clusters 1a (MNI) – IIa (TNV) and by R-mode clusters Ba (MNI) – βa (TNV). It is dominated by C. *torosa*, holoeuryhaline species commonly living in paralic environment. The benthic foraminifer species A. *aberdoveyensis* (lobate form), E. *poeyanum* (with depressed sutures) and *Haynesina germanica* and the ostracod species L. *elliptica* are characteristic taxa.

4.2.2.6. Core MSB. Two meiofaunal associations can be recognized in the Core MSB: a high energy, marine infralittoral association, characterized by benthic foraminiferal marine taxa, and a low diversity mesolittoral/supralittoral biofacies, dominated by poorly preserved benthic foraminiferal marine taxa.

4.2.2.7. Infralittoral marine association. This association, defined by Q-mode clusters 1b (MNI) – Ib (TNV), is characterized by autochthonous species such as *A. aberdoveyensis* (rounded form), A. *beccarii*, *B. granulata*, *B. aculeata*, *C. lobatulus, E. crispum* and the ostracod species *P. turbida*, all typical of infralittoral marine, relatively high energy waters. Reworked deep sea benthic foraminiferal species are very common.

4.2.2.8. Mesolittoral/supralittoral association. The association is defined by Q-mode clusters 2b (MNI) – IIb (TNV), and consists of benthic foraminiferal taxa provided of robust tests, in poor state of preservation. They pertain both to reworked taxa belonging to older sediments originally deposited in open sea waters, and to upper infralittoral species displaced by wave motion in the mesolittoral or supralittoral zone. The group of the infralittoral taxa is dominated by *A. aberdoveyensis* (rounded form) and *E. crispum*, whereas *C. carinata* and C. *pachyderma* dominates the reworked foraminiferal group. The diversity is very low. The delicate ostracod shells are lacking.

4.2.3. Paleoenvironments

4.2.3.1. Core MSA. The sediments collected in the core MSA yielded assemblages characterized by marine and brackish species. Considering the state of preservation of ostracod shells, the presence of young instars and adult ostracod specimens and their distribution data, marine infralittoral and paralic paleoenvironments have been inferred. The foraminiferal species typical of open shelf waters have been entirely considered allochthonous, reworked from Pliocene-Pleistocene pelitic sediments outcropping in the catchment area of the Basento River and transported by the river, whereas the upper infralittoral and brackish taxa have been mainly recognized as autochthonous. In the MSA core we have recognized the following intervals:

1. Samples MSA 33-MSA 11: assemblages characterized by marine taxa, with high abundances of reworked specimens. The autochthonous assemblages, including *Ammonia aberdoveyensis* “rounded form”, *Elphidium crispum*, *Pontocythere turbida*, indicate an upper infralittoral marine zone (i.e. upper shoreface);
2. Samples MSA 10-MSA 8: transitional phase, alternating upper mesolittoral-supralitoral (foreshore) levels, showing poorly preserved shallow-marine fossil remains, and brackish sediments;
3. Samples MSA 8-MSA 2: marginal paleoenvironment, linked to lagoonal and/or estuarine brackish waters. The autochthonous

Table 2
Semiquantitative distribution of microfossils remains (VR = very rare; R = rare; U = uncommon; C = common), benthic foraminiferal absolute abundance (I = individuals per 100 g of sediment), ostracod absolute abundance [I(MNI) = minimum number of individuals per 100 g of sediment; j indicates juvenile specimens] and ostracod absolute abundance [I(TNV) = total number of valves) per 100 g of sediment] from core MSB.

samples	MSB 33	MSB 31	MSB 29	MSB 28	MBS 26	MSB 24	MSB 21	MSB 19	MSB 16	MSB 14	MSB 12	MSB 11	MSB 10	MSB 9	MSB 8	MSB 6	MSB 4	MSB 2	MSB 1
meters	19.00	18.00	17.10	15.80	14.60	13.40	12.50	11.60	10.05	9.20	8.20	7.90	6.40	5.40	4.50	3.05	2.20	0.90	0.70
Bivalvia			R		R		U		VR		VR	VR	VR	R	VR				
Bryozoa										VR	VR							R	
Echinodermata		R	VR	VR	VR		VR	VR	VR	VR	U			VR				VR	
Foraminifera (planktonic)	R	U	R	C	C	R	VR	VR	C	U	C	VR	VR	VR	U	VR	R		VR
Gastropoda			R			R		U		R	VR	VR		R		R	R	U	R
Porifera	U	R	R	R	R	VR	VR	VR	VR	U	R			VR	VR	VR		VR	VR
Radiolaria										R						VR			VR
Foraminifera																			
Adelosina longirostra (d'Orbigny, 1826)	16			96	10			2			4								
Adelosina sp.	8																		
Ammodiscus planorbis Höglund, 1947					2														
Ammonia aberdoveyensis Haynes, 1973 lobate form			8	32	2														
Ammonia aberdoveyensis Haynes, 1973 rounded form	128	64	44	208	90	10	12	8	20	14	32	2	4	2	6	2			2
Ammonia beccarii (Linnaeus, 1758)	88	2	28	16	30			4	12	2	6			2					
Amphicoryna scalaris (Batsch, 1791)				32															
Amphistegina sp.										2	2								
Anomalinoides sp.					2														
Asterigerinata mamilla (Williamson, 1858)			4																
Astrononion stelligerum (d'Orbigny, 1839)			4	48							2								
Aubignyna perlucida (Heron-Allen and Earland, 1913)					2														
Bigenerina nodosaria d'Orbigny, 1826	8			16	4					2	2								
Bolivina alata (Seguenza, 1862)						2													
Bolivina catanensis Seguenza, 1862			4								2								
Brizalina spathulata (Williamson, 1858)	24	6	40	208	76				4										
Brizalina striatula (Cushman, 1922)			4																
Buccella granulata (Di Napoli Alliata, 1952)	8	10	16		6				12		8								
Bulimina aculeata d'Orbigny, 1826	80	34	48	336	72	2	2		8	6	10				2				
Bulimina elongata d'Orbigny, 1846	24	2	4	96	24										2				
Bulimina striata d'Orbigny, 1832			4	32					4										
Cassidulina carinata Silvestri, 1896	312	108	284	1568	364		4	18	64	20	64				2		4		4
Cibicides lobatulus (Walker & Jacob, 1798)	32	22	4	96	62	2		2	24	4	18				2	2			2
Cibicidoides robertsonianus (Brady, 1881)	8	12	8							4				2					
Cibicidoides pachyderma (Rzehak, 1886)	256	82	112	160	172	8	10	10	44	32	84	4	2	4	14	2	8	4	
Cycloforina contorta (d'Orbigny, 1846)				32	6														
Dentalina sp.	8		4																
Discorbinella bertheloti (d'Orbigny, 1839)		2		32	4														
Elphidium articulatum (d'Orbigny, 1839)	16				4														
Elphidium complanatum (d'Orbigny, 1839)			4																
Elphidium crispum (Linnaeus, 1758)	72	20	36	144	44	10	18	12	4	8	22	2		6	10			6	2
Elphidium granosum (d'Orbigny, 1826)	16	4	12		32						6								
Elphidium macellum (Fichtel & Moll, 1798)			8		2														
Elphidium poeyanum (d'Orbigny, 1839) FS form	24	2	8	32	16				8	6									
Elphidium punctatum (Terquem, 1878)		4	8	112	14				4	2	4								
Epistominella sp.											2								
Fissurina sp.					4														

(*continued on next page*)

Table 2 (*continued*)

samples	MSB 33	MSB 31	MSB 29	MSB 28	MBS 26	MSB 24	MSB 21	MSB 19	MSB 16	MSB 14	MSB 12	MSB 11	MSB 10	MSB 9	MSB 8	MSB 6	MSB 4	MSB 2	MSB 1
Globobulimina affinis (d'Orbigny, 1839)	8			48	4	2					2								
Globobulimina pseudospinescens (Emiliani, 1949)											2								
Globocassidulina subglobosa (Brady, 1881)		6	8	80	22					4						2			
Globulina gibba d'Orbigny, 1826								2											
Gyroidinoides soldanii (d'Orbigny, 1826)	8	6		80	8	2		2		2	2								
Gyroidinoides umbonata (Silvestri, 1898)				32	4														
Hoeglundina elegans (d'Orbigny, 1826)			12			2				2									
Hyalinea balthica (Schroeter, 1783)	8	4		80	18						2								
Laevidentalina sp.			4																
Lagena striata (d'Orbigny, 1839)					2														
Lenticulina cultrata (Montfort, 1808)			4																
Lenticulina inornata (d'Orbigny, 1846)	16	4			4			2		2			2	2					
Lenticulina orbicularis (d'Orbigny, 1826)			4																
Lenticulina sp.															2				
Marginulinopsis aff. *bradyi* (Goës, 1894)					2														
Martinottiella cylindrica (d'Orbigny, 1852)		2																	
Melonis affinis (Reuss, 1851)	48	20	20	256	62			2	8	8	12							2	4
Miliolinella subrotunda (Montagu, 1803)					2														
Neoconorbina terquemi (Rzehak, 1888)					10														
Nonion fabum (Fichtel & Moll, 1798)									4										
Oridorsalis umbonatus (Reuss, 1851)					2			4			2								
Planulina ariminensis d'Orbigny, 1826	32	6	8	32	22				8	2	6								
Pullenia bulloides (d'Orbigny, 1846)	24	8	4	16							2								
Pyrgo sp.				16															
Quinqueloculina bradyana Cushman, 1917			8																
Quinqueloculina padana Perconig, 1954	8	2		16	4						2								
Quinqueloculina seminulum (Linnaeus, 1758)	40		4	32	18			2			8								
Quinqueloculina viennensis Le Calvez and Le Calvez, 1958	72		24	128	34					4	2								
Quinqueloculina sp.					2	4													
Reussoolina apiculata (Reuss, 1851)		2																	
Rosalina floridana (Cushman, 1922)	8			16															
Sigmoilopsis schlumbergeri (Silvestri, 1904)				32	18	4		4										2	
Siphonaperta agglutinans (d'Orbigny, 1839)				16															
Siphonaperta aspera (d'Orbigny, 1826)					10														
Siphonaperta dilatata (Le Calvez and Le Calvez, 1958)	8	8	4	32						8	14								
Siphonina reticulata (Čžjžek, 1848)		2								2									
Siphonodosaria sp.					2				8										
Sphaeroidina bulloides d'Orbigny, 1826	16	6	32	112	24	2	4	2	4	4	2					2			
Spiroplectinella wrightii (Silvestri, 1903)	8				2														
Stainforthia complanata (Egger, 1893)					4														
Textularia agglutinans d'Orbigny, 1839			4																
Textularia calva Lalicker, 1935										4									
Textularia gramen d'Orbigny, 1846				32															
Textularia sp.					6														
Triloculina oblonga (Montagu, 1803)	8				4						2								
Triloculina schreibersiana d'Orbigny, 1839	40				10			2		2	4								
Triloculina trigonula (Lamarck, 1804)		2	8	48												2			
Uvigerina peregrina Cushman, 1923	208	42	40	976	158	2	2	4		6	18								
Valvulineria complanata (d'Orbigny, 1846)	24	18	32	784	112					2	4								

(*continued on next page*)

Table 2 (*continued*)

samples	MSB 33	MSB 31	MSB 29	MSB 28	MBS 26	MSB 24	MSB 21	MSB 19	MSB 16	MSB 14	MSB 12	MSB 11	MSB 10	MSB 9	MSB 8	MSB 6	MSB 4	MSB 2	MSB 1
species indeterminate		38	28		48				80	2	50			2	34				2
Ostracoda MNI																			
Aurila punctata (Münster, 1830)										2									
Aurila speyeri (Brady, 1868)										2									
Bosquetina rhodiensis Sissingh, 1972									4										
Carinocythereis whitei (Baird, 1850)					2														
Cimbaurila cimbaeformis (Seguenza, 1883)				j															
Cistacythereis turbida (G.W. Müller, 1894)				16															
Cytheretta adriatica Ruggieri, 1952				48															
Cytheridea neapolitana Kollmann, 1960				16	2														
Loxoconcha ovulata (Costa, 1853)				16	2														
Pontocythere turbida (G.W. Müller, 1894)	8		4	32 j	4					2									
Pterygocythereis jonesii (Baird, 1850)				j															
Semicytherura incongruens (G.W. Müller, 1894)									4										
Xestoleberis communis G.W. Müller, 1894																			2
Ostracoda TNV																			
Aurila punctata (Münster, 1830)										2									
Aurila speyeri (Brady, 1868)										4									
Bosquetina rhodiensis Sissingh, 1972									4										
Carinocythereis whitei (Baird, 1850)					2														
Cimbaurila cimbaeformis (Seguenza, 1883)				16															
Cistacythereis turbida (G.W. Müller, 1894)				16															
Cytheretta adriatica Ruggieri, 1952				80															
Cytheridea neapolitana Kollmann, 1960				32	4														
Loxoconcha ovulata (Costa, 1853)				16	2														
Pontocythere turbida (G.W. Müller, 1894)	8		4	80	4					2									
Pterygocythereis jonesii (Baird, 1850)				16															
Semicytherura incongruens (G.W. Müller, 1894)									4										
Xestoleberis communis G.W. Müller, 1894																			4

Table 3
Benthic foraminifer and ostracod abundances (Individuals) and simple diversity (Taxa).

core MSA																					
	MSA 33	MSA 32	MSA 30	MSA 28	MSA 26	MSA 23	MSA 21	MSA 18	MSA 16	MSA 14	MSA 13	MSA 11	MSA 10	MSA 9	MSA 8	MSA 7	MSA 6	MSA 5	MSA 4	MSA 3	MSA 2	MSA 1
Foraminifera																						
Taxa	46	43	39	40	31	35	44	44	32	38	40	37	4	12	5	11	9	29	4	3	5	1
Individuals	4160	5040	3888	2464	430	1480	2248	2456	1000	1240	956	1128	4	76	22	82	32	90	5	3	7	2
Ostracoda																						
Taxa	4	4	5	3	3	2	6	7	1	4	1	3		3		1	3	7	3	1	1	
Individuals	72	64	72	32	6	8	89	72	4	16	4	16		184		1	6	14	3	2	4	
MNI																						
Individuals TNV	128	96	104	32	8	8	112	120	4	16	4	28		1844		4	20	65	6	60	313	

core MSB																					
	MSB 33	MSB 31	MSB 29	MSB 28	MBS 26	MSB 24	MSB 21	MSB 19	MSB 16	MSB 14	MSB 12	MSB 11	MSB 10	MSB 9	MSB 8	MSB 6	MSB 4	MSB 2	MSB 1		
Foraminifera																					
Taxa	36	31	40	40	52	13	7	17	17	26	33	3	3	6	8	6	2	4	5		
Individuals	1712	512	916	6160	1614	52	52	82	240	154	354	8	8	18	40	12	12	14	14		
Ostracoda																					
Taxa	1		1	7	4				2	3									1		
Individuals MNI	8		4	130	10				8	6									2		
Individuals TNV	8		4	256	12				8	8									4		

assemblages are dominated by *Cyprideis torosa*, *Loxoconcha elliptica*, *Ammonia aberdoveyensis* "lobate form";

4. Sample MSA 1: the sample yielded a very poorly preserved assemblage, typical of emerged beach (foreshore-backshore), suggesting the record of a regressive peak.

In the intervals 2 and 3 the rare freshwater ostracod shells, possibly transported by the Basento River, testify the influx of continental waters during the deposition. The paleoenvironmental evolution evidences a relatively continuous, moderate regressive trend.

4.2.3.2. Core MSB. The fossil assemblages collected in the MSB core show the presence of two different paleoenvironments:

A) Samples MSB 33-MSB 12. Mixed assemblages with high abundances of allochthonous benthic foraminifers, whereas allochthonous ostracods are very rare. Diversity is moderately high. Upper infralittoral ostracods, dominated by *Pontocythere turbida*, are uncommon but well preserved. A deposition in an upper infralittoral zone (upper shoreface) with an high energy waters is inferred.

B) Samples MSB 11-MSB 1. The meiofaunal diversity is very low. Ostracods shells are not present (except few poorly preserved valves in the sample MSB 1). Benthic foraminiferal tests pertain to large taxa, show evidence of abrasion and are frequently damaged. They suggest a deposition in mesolittoral/supralittoral (foreshore) environment (emerged beach, dune).

The meiofaunal assemblages indicate that the two parts of the section represent two steps of a regression, shallow marine in the lower part and foreshore in the upper part.

5. Discussion

The analysis and interpretation of the different datasets obtained by the multidisciplinary study of the Metaponto Plain showed a rather complex morphological evolution of the area due to interactions between glacio-eustatic sea-level variations and tectonics. The analytic results and the stratigraphic correlations between the deposits from the two cores and marine terraces stratigraphy and ages allowed us to reconstruct the main depositional environments since the Late Pleistocene (Figs. 9 and 10).

As above quoted, the whole middle-late Pleistocene sequence of marine terraces and deposits is the most widespread class of geomorphological features in the study area and is the result of the interplay between regional tectonic uplift and global eustatic sea-level oscillations. Based on chronological constraints and related correlation between the inner edge of each terrace and the interglacial-interstadial peaks of the relative sea-level curve (Lisiecki and Raymo, 2005; Shackleton, 1987), eleven orders of marine terraces have been recognized in the investigated area (see Gioia et al., 2016, 2020; Gioia et al., 2018). The staircase of marine terraces ranges in elevation from 380 m a.s.l. to 10–15 m a.s.l. and each gently dipping surface is separated from the lower one by well-recognizable morphological scarps.

In the many studies focused on the marine terraces, the authors have interpreted the terrace sequence along the Taranto Gulf as having resulted from interactions between regional Quaternary land uplift and glacio-eustatic sea-level fluctuations. In add, Westaway and Bridgland (2007) investigated the rates and magnitudes of the Late Pliocene - Pleistocene uplift at key localities of Basilicata and Calabria using fluvial and marine terraces. They suggested a staircase of twelve marine terraces that formed during different marine highstands during the Pleistocene. They were consistent with the amino-acid dating evidence (e.g., Dai Pra and Hearty, 1988) and the 'Senegalese' fauna. Finally, the authors concluded that uplift rates show strong lateral variations, reaching

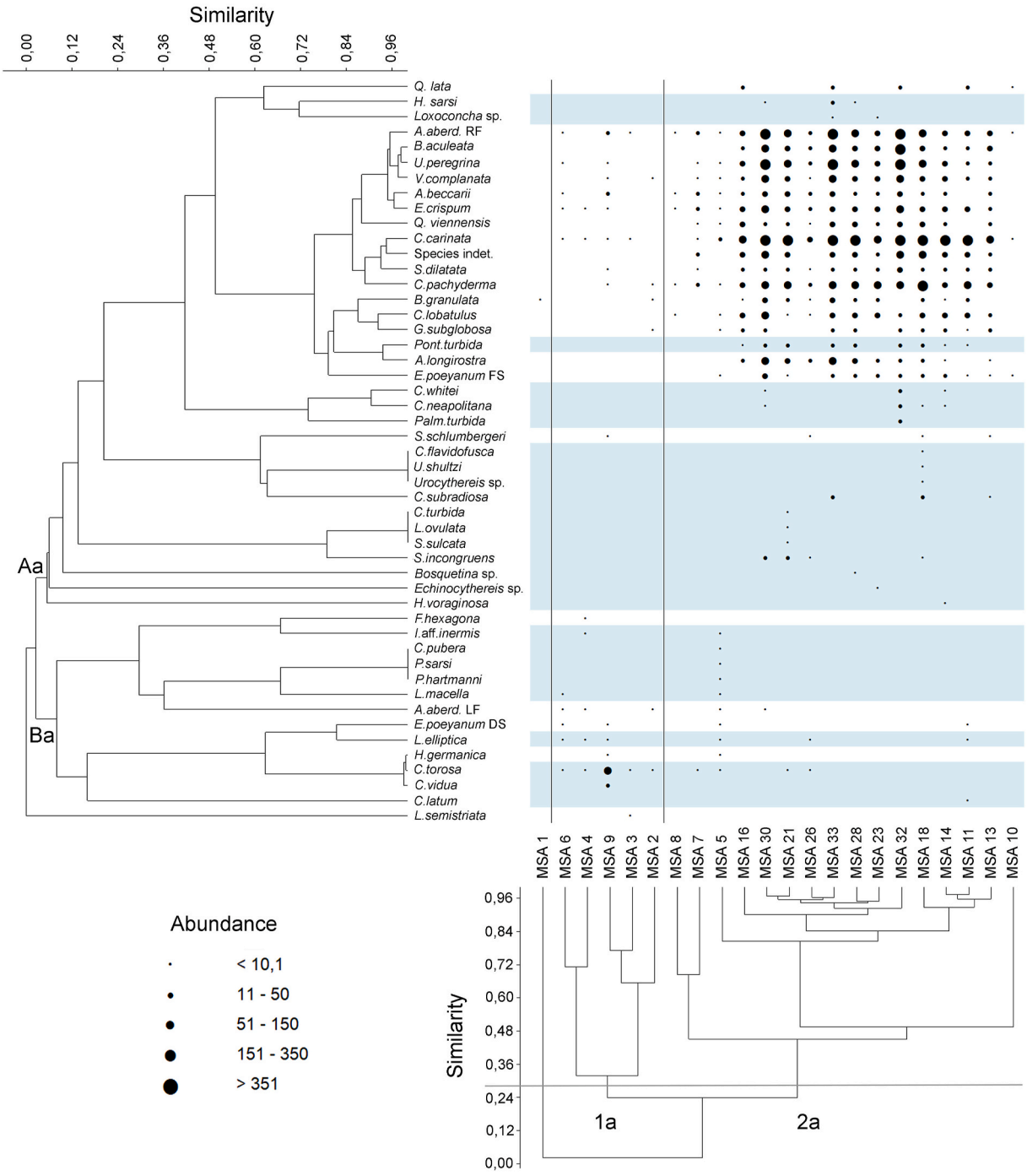

Fig. 4. Two-way cluster analysis based on foraminiferal and ostracod Minimal Number of Individuals for core MSA.

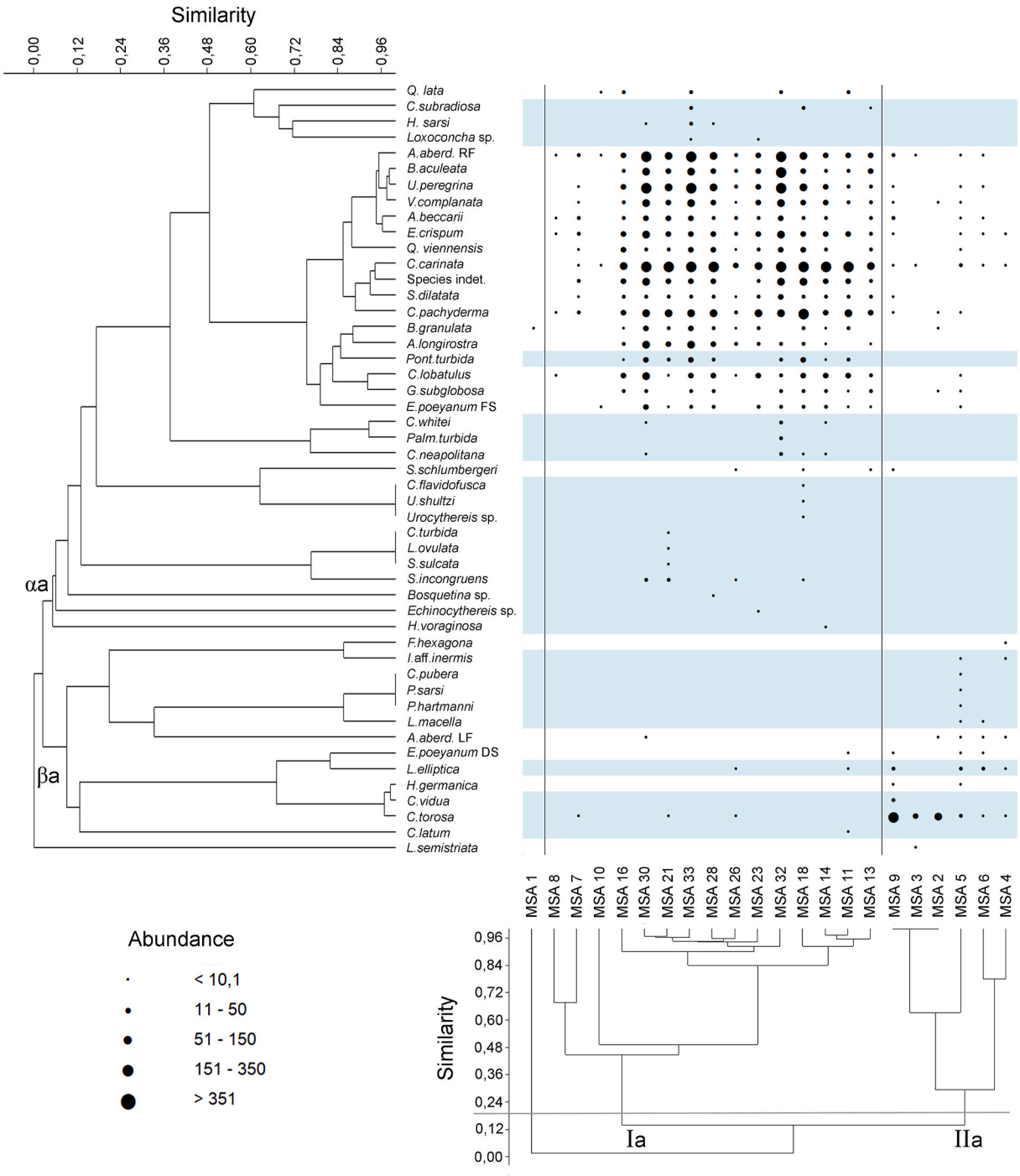

Fig. 5. Two-way cluster analysis based on foraminiferal and ostracod Total Number of Valves for core MSA.

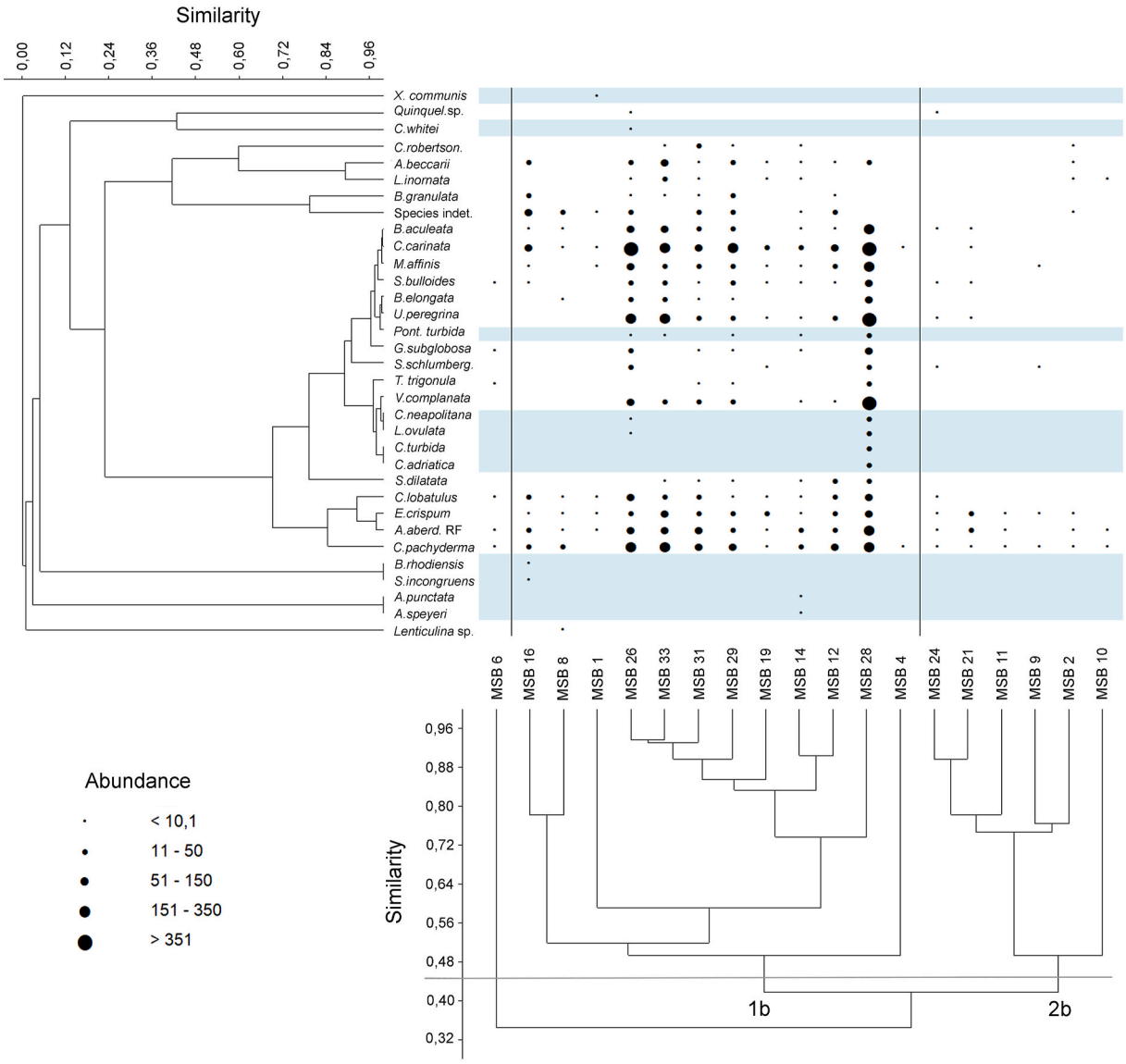

Fig. 6. Two-way cluster analysis based on foraminiferal and ostracod Minimal Number of Individuals for core MSB.

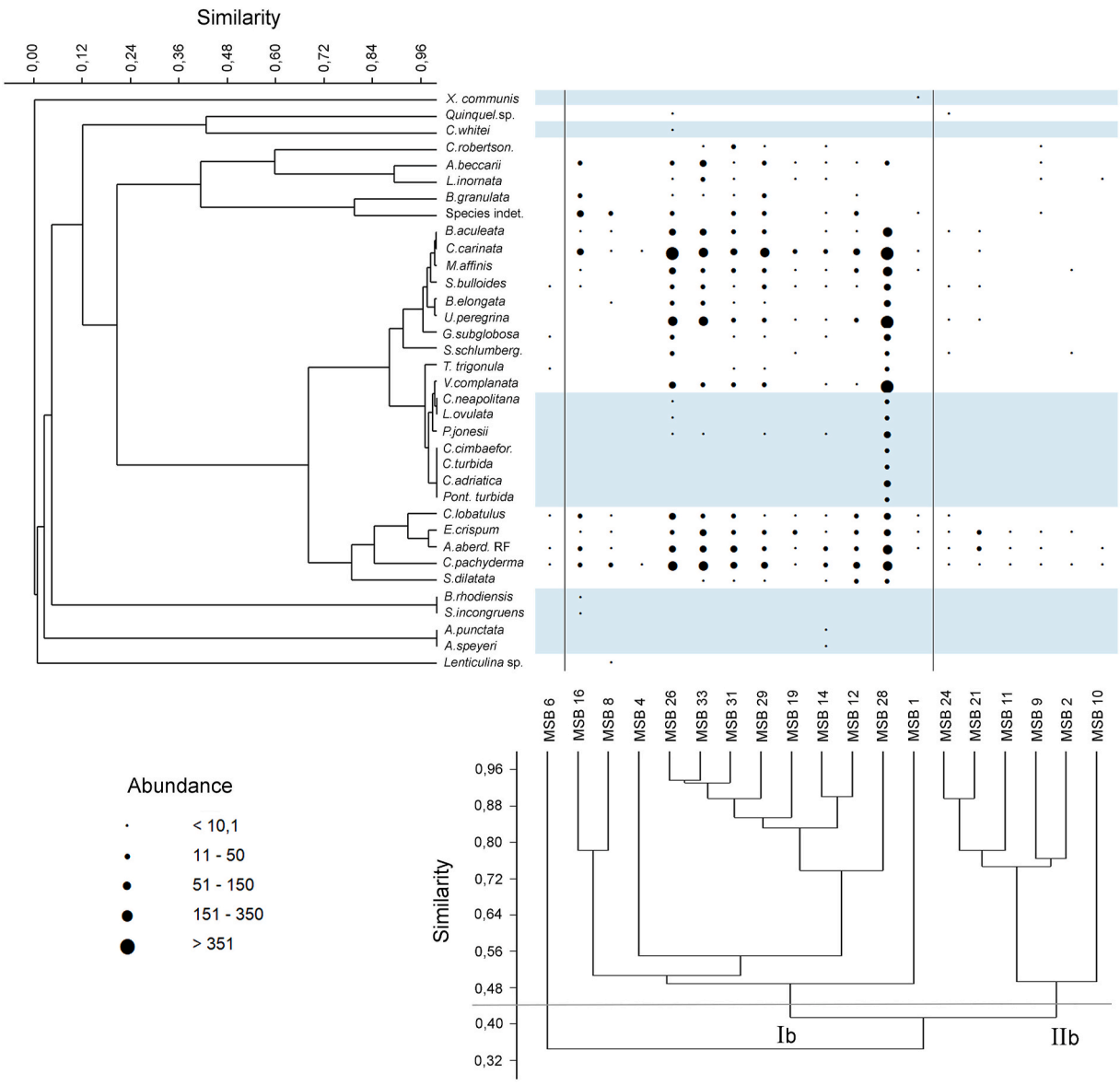

Fig. 7. Two-way cluster analysis based on foraminiferal and ostracod Total Number of Valves for core MSB.

maxima of 1 mm/yr or more in the southern Apennines, and a maximum value of ca. 0.55 mm/a at the Pisticci marine terrace staircase.

In this work, the ages of most of the terraces and their associations with highstands have been inferred based on dated terraces: Policoro (Belluomini et al., 2002; Brückner, 1980; Dai Pra and Hearty, 1988; Zander et al., 2006), Metaponto 3 (not present in our study area; see Caputo et al., 2010), San Teodoro (Belluomini et al., 2002; Zander et al., 2006), and San Basilio (Belluomini et al., 2002; Dai Pra and Hearty, 1988; Zander et al., 2006). More recently, Gioia et al. (2016) and Gioia et al. (2020) recognized eleven marine terraces (MT1 to MT11 from the youngest to the oldest) and inferred their ages using a critical revision of the chronological data that are available in the literature.

Considering only the most recent marine terraces (i.e., starting from MIS 5.5 and their respective altitude), we compared them to the sea-level variation curve by Benjamin et al. (2017). The MIS 5.5 terrace is located at an average altitude of about 80 m a.s.l., the MIS 5.3 terrace at an average altitude of about 65 m a.s.l., the MIS 5.1 terrace at 30 m a.s.l., and the MIS 3 terrace at about 15 m a.s.l.; therefore, all the marine terraces have a higher altitude than expected: those referred to the MIS 5.5 and MIS 5.3 exceed the quote of about 80 meters, whereas the MIS 5.1 and MIS 3 one is about 65 m above the expected elevation (Fig. 9).

Both the boreholes have a marine succession at the base (more precisely referable to the upper infralittoral marine environment) deposited during MIS 3 (stratigraphic unit U1). A clay interval (mesolittoral/supralittoral), about 2 m-ticks and referring to the U2 unit (~15 cal yr BP), in the MSA well overlaps this basal marine unit. Furthermore, at the top of the U2 unit, there is a lagoon and/or estuary unit (U3) with a thickness of about 5 meters in the MSA well whereas in the MSB well this unit is absent. At the top of the MSB borehole, the U4b Unit of mesolittoral/infralittoral environment, with a thickness of about 8.5 meters, can be correlated to the U4a unit of foreshore-backshore environment from the MSA core.

It is worth noting that the environmental characteristics deduced from the sediments of the MSB well indicate a greater proximity of those paleoenvironments to the coastline and to the bed of the Basento River respect to the coeval deposits from the MSA well.

The depths and ages of the marine indicators from the two wells can be compared with the sea-level variation curves of Benjamin et al. (2017) for the Late Pleistocene and Lambeck et al. (2011) for the Holocene. The sample LTL14791A, referred to MIS 3 (33,189.5 ± 517.5 cal yr BP), is found at −10.60 meters a.s.l., about 65 meters higher than the expected depth. The sample LTL14795A is located at −6.55 m a.s.l. and

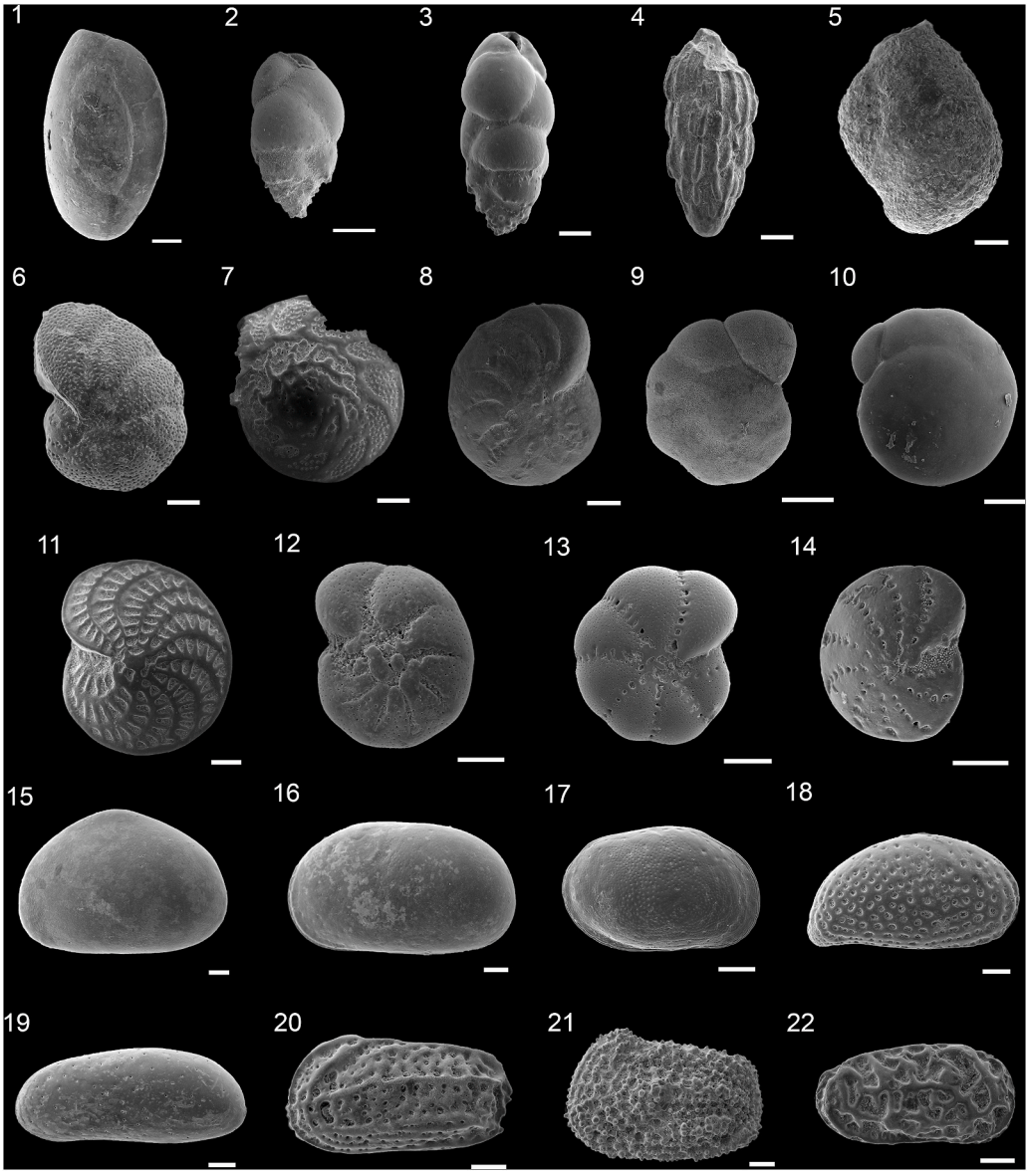

Fig. 8. 1. *Quinqueloculina seminulum* (Linnaeus, 1758), four chamber side, sample MSA 28, ABMC 2021/017; **2.** *Bulimina aculeata* d'Orbigny, 1826, lateral view, sample MSA 33, ABMC 2021/013; **3.** *Bulimina elongata* d'Orbigny, 1846, lateral view, sample MSB 28, ABMC 2021/009; **4.** *Uvigerina peregrina* Cushman, 1923, lateral view, sample MSA 30, ABMC 2021/008; **5.** *Siphonaperta agglutinans* (d'Orbigny, 1839), side view sample MSA 21, ABMC 2021/006; **6.** *Cibicides lobatulus* (Walker & Jacob, 1798), spiral side, sample MSA 30, ABMC 2021/016; **7.** *Cibicidoides pachyderma* (Rzehak, 1886), spiral side, sample MSA 26, ABMC 2021/012; **8.** *Astrononion stelligerum* (d'Orbigny, 1839), side view, sample MSA 11, ABMC 2021/004; **9.** *Ammonia aberdoveyensis* Haynes, 1973 lobate form, spiral side, sample MSA 6, ABMC 2021/010; **10.** *Ammonia aberdoveyensis* Haynes, 1973 rounded form, spiral side, sample MSA 29, ABMC 2021/015; **11.** *Elphidium crispum* (Linnaeus, 1758), side view, sample MSA 29, ABMC 2021/019; **12.** *Elphidium granosum* (d'Orbigny, 1826), side view, sample MSA 11, ABMC 2021/014; **13.** *Elphidium poeyanum* (d'Orbigny, 1839) DS form, side view, sample MSA 6, ABMC 2021/007; **14.** *Elphidium punctatum* (Terquem, 1878), side view, sample MSB 28, ABMC 2021/011; **15.** *Cypridopsis vidua* (O.F. Müller, 1776), left valve, sample MSA 9, ABMC 2021/025; **16.** *Cyprideis torosa* (Jones, 1850), left valve, female, sample MSA 9, ABMC 2021/024; **17.** *Loxoconcha elliptica* Brady, 1868, right valve, female, sample MSA 6, ABMC 2021/026; **18.** *Cytheridea neapolitana* Kollmann, 1960, right valve, sample MSB 26, ABMC 2021/021; **19.** *Pontocythere turbida* (G. W. Müller, 1894), left valve, sample MSA 33, ABMC 2021/022; **20.** *Cistacythereis turbida* (G.W. Müller, 1894), left valve, sample MSA 21, ABMC 2021/023; **21.** *Heryhowella sarsi* (G.W. Müller, 1894), left valve, sample MSA 30, ABMC 2021/027; **22.** *Callistocythere flavidofusca* (Ruggieri, 1950), right valve, sample MSA 18, ABMC 2021/020. Scale bar = 100 μm.

furnished an age of 14,885.5 ± 379.5 whereas the sample LTL14796A at −6.80 m a.s.l. gave an age of 15,755.5 ± 299.5. These latter samples are marine points and located about 65 meters above the expected ancient sea level, as well. The sample LTL14789A from the MSB well, taken at −5.15 m a.s.l. and dated at 3742 ± 45 years BP, is located 3 m below (Fig. 10) the expected height from the curve of Lambeck et al. (2011).

On this basis, the Late Quaternary paleoenvironmental evolution of the Metaponto coastal plain can be summarized as follows.

During MIS 5.5 and MIS 5.3 two marine terraces formed: for both, the differences of the heights of internal edges respect the paleo sea levels is the same (i.e., about 80 meters, Fig. 9). Therefore, it can be assumed that in that time span the study area was characterized by tectonic stability (Figs. 9 and 11). The MIS 5.1 and MIS 3 highstands are witnessed by two terraces whose heights are both about 65 m above the expected paleolevel, a difference comparable to that of the sea-level indicators from the well deposits. In this case, it can be assumed that the surface underwent a tectonic uplift of at least 15 meters between MIS 5.3 and MIS 5.1, followed by tectonic stability up to 15,000 yr BP at least. After this period of stability, the study area was affected by a strong uplift of about 65 meters, which represents the highest value recorded until now. On the other hand, data from the MSB core, relative to a difference of about 3 m between the marine point indicated by sediments analyses and the comparison curve, suggest that the uplift stopped at about 3–4 kyr BP. So, such a difference in heights may be due to a possible younger subsidence phenomenon probably linked to the compaction of alluvial and lagoon deposits (Figs. 3, 10 and 12), as already detected in different coastal plains of southern Italy (Polcari et al., 2018; Matano, 2019; Amato et al., 2020).

Another morphological element that can be here used as a constraint is the continental shelf. In fact, during the Quaternary, the Mediterranean continental shelves, due to their relative low depth, underwent many emersion cycles provoked by glaciation-induced sea-level falls (Benjamin et al., 2017). These changes were responsible for the current morphology of the shelves, since their margins mostly coincide with the minimum height reached by the sea during the last glacial maximum (LGM, ca. −120 m a.s.l.). In the study area, the depth of the shelf edge is at about −50 m a.s.l. (Fig. 1), ca. 70 m above the expected height (Fig. 9). Such a value is comparable to the amount of uplift (ca. 65 m) calculated for the more recent terraces and marine markers from cores. Therefore, it seems reasonable that recent and relevant vertical movements due to regional tectonics must be added to the eustatic changes acting on a global scale to fully explain the evolutionary history of the Metaponto Plain. This uplift could be attributed to a general – maybe still active –bending of the foredeep area due to the propagation toward east-northeast and south-east, respectively, of blind thrusting of the Campania-Lucania and Calabrian segments of the southern Apennines chain, as already inferred by Caputo et al. (2010) and Gioia et al. (2018) on the basis of subtle geomorphological evidence of marine terrace staircase deformation and drainage network modification.

Several multidisciplinary works have investigated the plano-altimetric distribution of deformed marine terrace staircase along the Ionian coast of southern Italy, highlighting a general and decreasing trend of Middle-Upper Pleistocene tectonic uplift from about 0.2 to 0.3 mm/yr in the northern sectors to almost 2 mm/yr in the southern ones (Caputo et al., 2010; Santoro et al., 2013). Lateral and vertical distribution of marine terraces also indicated the occurrence of differential uplift and local tilting phenomena along the NE-SW direction, which can be ascribed to the late Quaternary activity of blind thrusts with a scarce/subtle morphological evidence (Caputo et al., 2010; Santoro et al., 2013). More recently, Gioia et al. (2018) infer a possible active tectonic control on drainage network geometry of the central sector of the Metaponto plain (i.e from Basento to Cavone rivers) driven by folding due to the late Quaternary activity of the blind thrust of the southern Apennines chain. Our multidisciplinary data seem to confirm the relevant role of active and episodic deformation induced by buried thrust front on the Late Quaternary evolution of the Metaponto plain, suggesting also an alternation of stages of severe tectonic uplift and periods of slower or null deformation.

The most recent evolution of the study area is characterized by, starting from the last 7000–8000 years, a slow and constant migration seaward of the shoreline (Fig. 1). The position of the shoreline during the last 3000 years has been reconstructed by both archaeological and topographic data. Archaeological evidence (i.e., the presence of remnants ascribed to *horrea*; Giardino, 1991 and references therein) combined to the results of our geomorphological survey (e.g., reconstruction of the landforms related to the Basento paleo-mouth) allowed us to infer that the ancient Port of Metapontum (8th-7th century B.C.) was likely located in Santa Pelagina area, close to a reclaimed coastal pond, at ca. 1.5 km from the present shoreline. Furthermore, the quadrangular watchtowers built at the end of the 16th century along the shoreline are now located about 1 km inland, suggesting a progradation of the shoreline of ca. 500 m since the 8th-7th century B.C. This progradational trend proceeded until the second half of the 20th century, with rates of ca. 4 m/yr during the time interval 1873–1954, based on both the historical and recent topographic maps of the area.

The seaward migration of the Metaponto Plain coastline ended starting from the second half of the last century, when dam construction on rivers and sediment exploitation from riverbeds caused severe coastal erosion, resulting in the retreat of the shoreline (Cocco et al., 1976; Sabato et al., 2012).

Quaternary morpho-stratigraphic evolution of the Metaponto plain resulting from the complex interplay between regional and fault-induced uplift and eustatic sea-level changes is undoubtedly different than the recent evolution of other coastal plains of the Ionian belt of southern Italy. The recent evolution of the northern Calabria ionian sector between Corigliano and Capo Trionto was reconstructed by Molin et al. (2002), Carobene (2003) and Robustelli et al. (2009) on the basis of morphological and sedimentary analysis of terraced surfaces. The authors infer a decreasing of Middle Pleistocene-Holocene uplift rates from about 1 mm/y in the westernmost sector to 0.46–0.69 mm/y to the east. Morphotectonic analyses of the Sibari coastal plain highlight a long-term history of tectonic uplift since Middle Pleistocene with a rate of about 1 mm/yr (Ferranti et al., 2011). Holocene evolution of the Sybaris archaeological site shows a well-constrained rapid subsidence, which has been interpreted as the result of local-scale tectonic signal and sediment compaction (Ferranti et al., 2011). In Monaco et al. (2002), morphological data suggest that eastern Sicily has been affected by an acceleration of uplifting since the Middle Pleistocene. The process activated in the foreland sector and migrated northward, towards the mountain belt. In the foreland area, the uplift increase started at 300–400 kyr with rates of 0.65 mm/yr, and was related to normal faulting in the Ionian offshore. At the front of the chain (Catania-Aci Trezza area), an increasing in the uplift rate occurred since about 200 kyr, corresponding to the end of the contractional tectonic regime responsible for the late stages of evolution of the eastern Sicilian thrust-system. The uplift, characterised by rate (~1.3 mm/yr), comparable to that reported by Gillot et al. (1994) for the Catania area since the Middle Pleistocene (1.1–1.6 mm/yr), relates to the northward propagation of the normal faulting to the Etnean area about 200 kyr ago (Monaco et al., 1997).

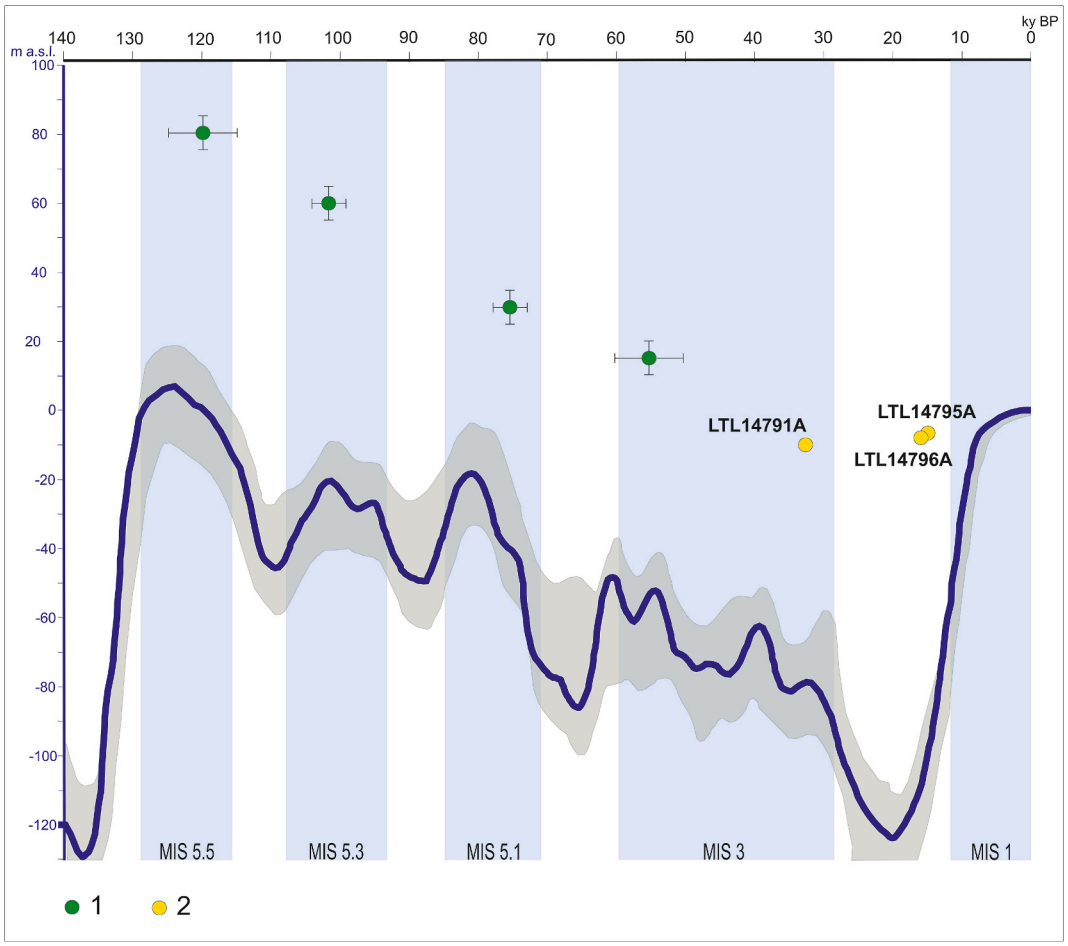

Fig. 9. Global mean sea-level curve with uncertainty indicated in grey (Benjamin et al., 2017). (1) elevation of the marine terrace; (2) depth of marine deposits in borehole.

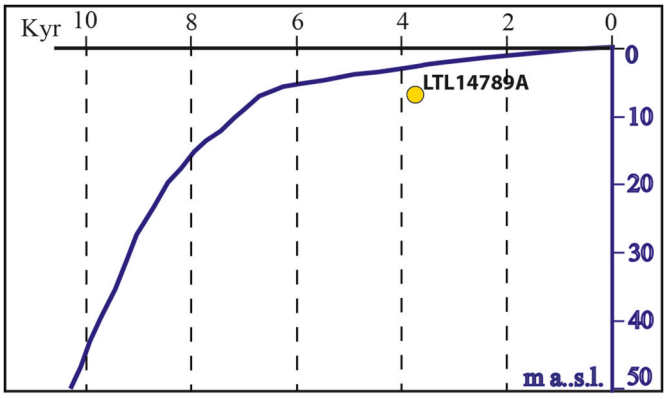

Fig. 10. Eustatic and glacio-hydro-isostatic curve of the Holocene with the data relating to the marine deposits of the MSB well.

6. Conclusions

The analyses of Quaternary deposits from two boreholes, both about 20 m-deep, drilled in the northern part of the Metaponto Plain, and geomorphological observations on marine terraces at the back of the coastal plain furnished helpful information about tectonic activity and sea-level changes occurred in that coastal-alluvial environment. The results, obtained by a multidisciplinary approach, suggest a new detailed evolutionary path of the coastal area, articulated into different steps. In particular, the Late Quaternary evolution of this plain as already known in literature is characterized by uplift rates showing strong lateral variations, reaching a maximum value of 1 mm/yr or more in the southern Apennines and a maximum value of ca. 0.55 mm/yr at the Pisticci marine terrace staircase.

The data used in this paper, relating to the terraces starting from MIS 5.5 and the ones coming from the core analyses, would seem to define that between the MIS 5.5 and the MIS 5.3 there is a stage of tectonic rest, and that the genesis of the terraces is mainly conditioned by eustatic variations. After MIS 5.3 there should be a stage of tectonic uplift of about 15 meters in 25 kyr, which allows us to identify an average uplift rate of 0.6 mm/yr. Subsequently, the present-day altitude of the marine terraces and the depth of the marine deposits in borehole and of the continental shelf of the Taranto Gulf allow us to define that between MIS 5.1 ("Neotyrrhenian" *Auctt.*) and 15,000 years BP there would seem to be another period of tectonic stability, followed by another phase of tectonic uplift between 15,000 years BP and more recent times, with a very high value of uplift rate (about 4 mm/yr). Our reconstruction identifies the recent/present rising of the coastal plain of Metaponto, indicates that the distribution of the uplift through the time is concentrated in some specific chronological intervals and, above all, that a strong and unsuspected increase of uplift rates occurred in the last part of the Late Pleistocene and in the Holocene.

Author contributions

G.C., P.D.L., D.G, A.M.A. and M.S performed the geomorphological, stratigraphical and geoarchaeological analyses, G.A., D.B., and R.P

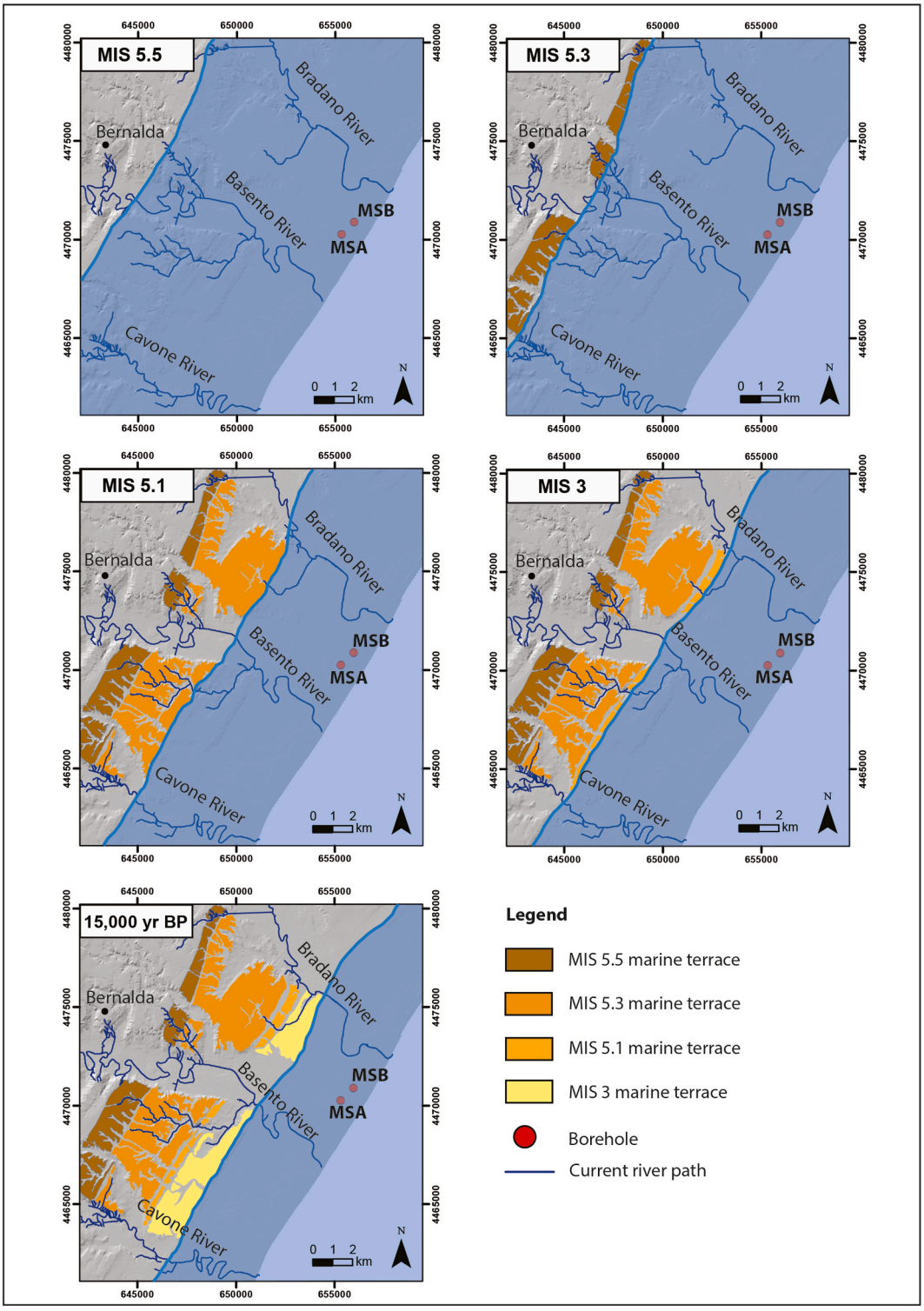

Fig. 11. Metaponto Plain paleogeographical sketches from MIS 5.5–15 kyr BP, showing the supposed shoreline position and some paleoenvironmental interpretations.

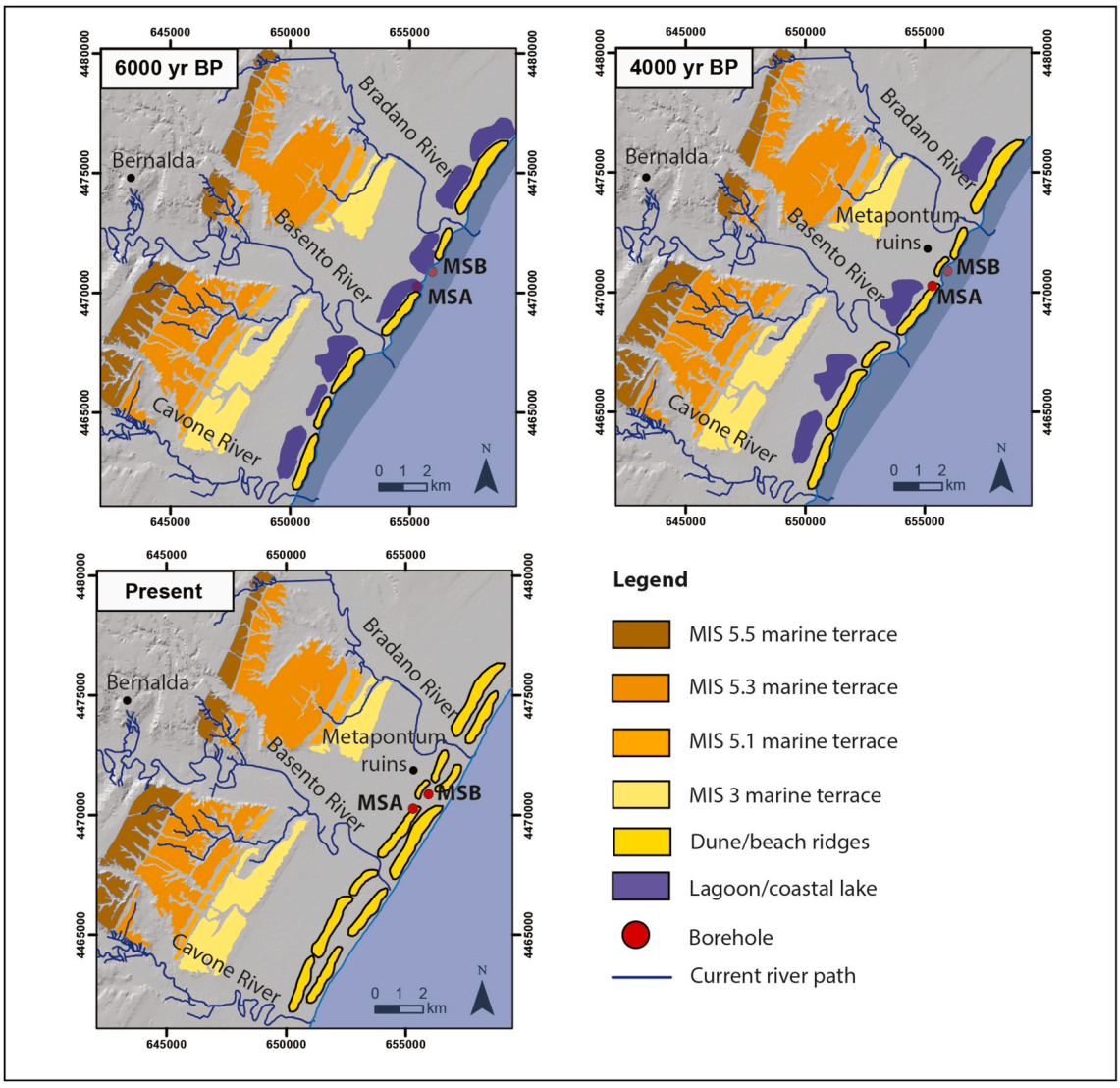

Fig. 12. Metaponto Plain paleogeographical sketches from 6 kyr BP to the present-day, showing the supposed shoreline position and some paleoenvironmental interpretations.

analysed the borehole samples and carried out the palaeoecological interpretation. All the Authors contributed to the conceptualization, design and implementation of the research, to the analysis of the results and to the writing of the manuscript.

Data availability

The authors confirm that the data supporting the findings of this study are available within the article and its supplementary materials.

Declaration of competing interest

The authors declare that they have no known competing financial interests or personal relationships that could have appeared to influence the work reported in this paper.

Appendix A. Supplementary data

Supplementary data to this article can be found online at https://doi.org/10.1016/j.quaint.2022.01.008.

APPENDIX 1. Benthic foraminifer and ostracod list of species

● Marine species reworked from Plio-Pleistocene outcrops
●● Freshwater species
List of benthic foraminiferal species
Adelosina elegans (Williamson, 1858)
Adelosina longirostra (d'Orbigny, 1826)
Adelosina mediterranensis (Le Calvez & Le Calvez, 1958)
Adelosina sp
Ammodiscus planorbis Höglund, 1947 ●
Ammonia aberdoveyensis Haynes, 1973 lobate form
Ammonia aberdoveyensis Haynes, 1973 rounded form
Ammonia beccarii (Linnaeus, 1758)
Amphicoryna scalaris (Batsch, 1791) ●
Amphistegina sp
Anomalinoides sp. ●
Asterigerinata mamilla (Williamson, 1858)
Astrononion stelligerum (d'Orbigny, 1839)
Aubignyna perlucida (Heron-Allen & Earland, 1913)
Bigenerina nodosaria d'Orbigny, 1826 ●
Bolivina alata (Seguenza, 1862) ●
Bolivina catanensis Seguenza, 1862 ●

Brizalina spathulata (Williamson, 1858) ●
Brizalina striatula (Cushman, 1922)
Buccella granulata (Di Napoli Alliata, 1952)
Bulimina aculeata d'Orbigny, 1826
Bulimina elongata d'Orbigny, 1846
Bulimina striata d'Orbigny, 1832 ●
Cassidulina carinata Silvestri, 1896 ●
Cibicides lobatulus (Walker & Jacob, 1798)
Cibicidoides bradyi (Trauth, 1918) ●
Cibicidoides pachyderma (Rzehak, 1886) ●
Cibicidoides robertsonianus (Brady, 1881) ●
Cibicidoides variabilis (d'Orbigny, 1826)
Cornuspira involvens (Reuss, 1850) ●
Cycloforina contorta (d'Orbigny, 1846)
Cycloforina villafranca (Le Calvez & Le Calvez, 1958) ●
Dentalina sp. ●
Discorbinella bertheloti (d'Orbigny, 1839) ●
Elphidium articulatum (d'Orbigny, 1839)
Elphidium complanatum (d'Orbigny, 1839)
Elphidium crispum (Linnaeus, 1758)
Elphidium granosum (d'Orbigny, 1826)
Elphidium macellum (Fichtel & Moll, 1798)
Elphidium poeyanum (d'Orbigny, 1839) DS form
Elphidium poeyanum (d'Orbigny, 1839) FS form
Elphidium pulvereum Todd, 1958
Elphidium punctatum (Terquem, 1878)
Epistominella sp. ●
Favulina hexagona (Williamson, 1848) ●
Fissurina orbignyana Seguenza, 1862 ●
Fissurina spp. ●
Globobulimina affinis (d'Orbigny, 1839) ●
Globobulimina pseudospinescens (Emiliani, 1949) ●
Globocassidulina subglobosa (Brady, 1881) ●
Globulina gibba d'Orbigny, 1826
Gyroidinoides soldanii (d'Orbigny, 1826) ●
Gyroidinoides umbonata (Silvestri, 1898) ●
Haynesina germanica (Ehrenberg, 1840)
Hoeglundina elegans (d'Orbigny, 1826) ●
Hyalinea balthica (Schroeter, 1783) ●
Laevidentalina sp. ●
Lagena striata (d'Orbigny, 1839) ●
Lagena semistriata Williamson, 1848 ●
Lenticulina cultrata (Montfort, 1808) ●
Lenticulina inornata (d'Orbigny, 1846) ●
Lenticulina orbicularis (d'Orbigny, 1826) ●
Lenticulina sp. ●
Marginulinopsis aff. *bradyi* (Goës, 1894) ●
Marginulinopsis costata (Batsch, 1791) ●
Martinottiella cylindrica (d'Orbigny, 1852) ●
Melonis affinis (Reuss, 1851) ●
Miliolinella subrotunda (Montagu, 1803)
Neoconorbina terquemi (Rzehak, 1888) ●
Nonion fabum (Fichtel & Moll, 1798).
Oridorsalis umbonatus (Reuss, 1851) ●
Planulina ariminensis d'Orbigny, 1826 ●
Pseudoclavulina crustata Cushman, 1936●
Pullenia bulloides (d'Orbigny, 1846) ●
Pyrgo inornata (d'Orbigny, 1846) ●
Pyrgo sp. ●
Quinqueloculina bradyana Cushman, 1917
Quinqueloculina lata Terquem, 1876
Quinqueloculina padana Perconig, 1954 ●
Quinqueloculina pygmaea Reuss, 1850
Quinqueloculina seminulum (Linnaeus, 1758)
Quinqueloculina viennensis Le Calvez & Le Calvez, 1958 ●
Quinqueloculina sp. ●
Reussella spinulosa (Reuss, 1850) ●
Reussoolina apiculata (Reuss, 1851) ●
Rosalina floridana (Cushman, 1922)
Sigmoilopsis schlumbergeri (Silvestri, 1904) ●
Siphonaperta agglutinans (d'Orbigny, 1839)
Siphonaperta aspera (d'Orbigny, 1826)
Siphonaperta dilatata (Le Calvez & Le Calvez, 1958)
Siphonina reticulata (Čžjžek, 1848) ●
Siphonodosaria sp. ●
Sphaeroidina bulloides d'Orbigny, 1826 ●
Spiroloculina depressa d'Orbigny, 1826
Spiroplectinella wrightii (Silvestri, 1903) ●
Stainforthia complanata (Egger, 1893)
Textularia agglutinans d'Orbigny, 1839 ●
Textularia calva Lalicker, 1935 ●
Textularia gramen d'Orbigny, 1846 ●
Textularia sp. ●
Triloculina eburnea d'Orbigny, 1839
Triloculina oblonga (Montagu, 1803) ●
Triloculina plicata Terquem, 1878
Triloculina schreibersiana d'Orbigny, 1839
Triloculina trigonula (Lamarck, 1804)
Uvigerina peregrina Cushman, 1923 ●
Uvigerina sp. ●
Valvulineria complanata (d'Orbigny, 1846) ●
List of ostracod species
Aurila punctata (Münster, 1830)
Aurila speyeri (Brady, 1868)
Bosquetina rhodiensis Sissingh, 1972 ●
Bosquetina sp. ●
Callistocythere flavidofusca (Ruggieri, 1950)
Carinocythereis whitei (Baird, 1850)
Cimbaurila cimbaeformis (Seguenza, 1883)
Cistacythereis turbida (G.W. Müller, 1894)
Cyprideis torosa (Jones, 1850)
Cypridopsis vidua (O.F. Müller, 1776) ●●
Cypris pubera O.F. Müller, 1776 ●●
Cytheretta adriatica Ruggieri, 1952
Cytheretta subradiosa (Roemer, 1838)
Cytheridea neapolitana Kollmann, 1960
Cytheropteron latum G.W. Müller, 1894 ●
Echinocythereis sp. ●
Henryhowella sarsi (G.W. Müller, 1894) ●
Heterocythereis voraginosa Athersuch, 1979
Ilyocypris aff. *inermis* Kaufmann, 1900 ●●
Leptocythere macella Ruggieri, 1975
Loxoconcha elliptica Brady, 1868
Loxoconcha ovulata (Costa, 1853)
Loxoconcha sp.
Palmoconcha turbida (G.W. Müller, 1894)
Pontocythere turbida (G.W. Müller, 1894)
Pseudocandona sarsi (Hartwig, 1899) ●●
Pseudolimnocythere hartmanni Danielopol, 1979
Pterygocythereis jonesii (Baird, 1850)
Semicytherura incongruens (G.W. Müller, 1894)
Semicytherura sulcata (G.W. Müller, 1894)
Urocythereis schultzi (Hartmann, 1958)
Urocythereis sp.
Xestoleberis communis G.W. Müller, 1894

References

Abate, D., De Pippo, T., Ilardi, M., Pennetta, M., 1998. Studio delle caratteristiche morfoevolutive quaternarie della piana del Garigliano. Il Quat. 11, 149–158.
Aiello, G., Amato, V., Aucelli, P.P.C., Barra, D., Corrado, G., Di Leo, P., Di Lorenzo, H., Jicha, B., Pappone, G., Parisi, R., Petrosino, P., Russo Ermolli, E., Schiattarella, M., 2021a. Multiproxy study of cores from the Garigliano plain: an insight into the late

quaternary coastal evolution of central-southern Italy. Palaeogeography, palaeoclimatology. Palaeoecology 567, 110298.
Aiello, G., Amato, V., Barra, D., Caporaso, L., Caruso, T., Giaccio, B., Parisi, R., Rossi, A., 2020. Late Quaternary benthic foraminiferal and ostracod response to palaeoenvironmental changes in a Mediterranean coastal area, Port of Salerno, Tyrrhenian Sea. Regional Studies in Marine Science 40, 101498.
Aiello, G., Barra, D., 2010. Crustacea, Ostracoda. Biol. Mar. Mediterr. 17, 401–419.
Aiello, G., Barra, D., Coppa, M.G., Valente, A., Zeni, F., 2006. Recent infralittoral foraminiferida and Ostracoda from the Porto Cesareo lagoon (Ionian Sea, mediterranean). Boll. Soc. Paleontol. Ital. 45, 1–14.
Aiello, G., Barra, D., De Pippo, T., Donadio, C., 2012. Pleistocene foraminiferida and Ostracoda from the island of Procida (Bay of Naples, Italy). Boll. Soc. Paleontol. Ital. 51, 49–62.
Aiello, G., Barra, D., De Pippo, T., Donadio, C., Miele, P., Russo Ermolli, E., 2007. Morphological and paleoenvironmental evolution of the Vendicio coastal plain in the Holocene (Latium, Central Italy). Il Quat. 20, 185–194.
Aiello, G., Barra, D., Parisi, R., Arienzo, M., Donadio, C., Ferrara, L., Toscanesi, M., Trifuoggi, M., 2021b. Infralittoral Ostracoda and benthic foraminifera of the Gulf of Pozzuoli (Tyrrhenian sea, Italy). Aquat. Ecol. 55, 955–998.
Aiello, G., Barra, D., Parisi, R., Isaia, R., Marturano, A., 2018. Holocene benthic foraminiferal and ostracod assemblages in a paleo-hydrothermal vent system of Campi Flegrei (Campania, South Italy). Palaeontol. Electron. 21 (3.41A), 1–71.
Aiello, G., Barra, D., Parisi, R., 2015. Lower-middle Pleistocene ostracod assemblages from the Montalbano Jonico section (Basilicata, southern Italy). Quat. Int. 383, 47–73.
Amato, V., Aucelli, P.P.C., Corrado, G., Di Paola, G., Matano, F., Pappone, G., Schiattarella, M., 2020. Comparing geological and Persistent Scatterer Interferometry data of the Sele River coastal plain, southern Italy: implications for recent subsidence trends. Geomorphology 351, 106953.
Antonioli, F., Anzidei, M., Amorosi, A., Lo Presti, V., Mastronuzzi, G., Deiana, G., De Falco, G., Fontana, A., Fontolan, G., Lisco, S., Marsico, A., Moretti, M., Orrù, P.E., Sannino, G.M., Serpelloni, E., Vecchio, A., 2017. Sea-level rise and potential drowning of the Italian coastal plains: flooding risk scenarios for 2100. Quat. Sci. Rev. 158, 29–43.
Aucelli, P.P.C., Amato, V., Budillon, F., Senatore, M.R., Amodio, S., D'Amico, C., Da Prato, S., Ferraro, L., Pappone, G., Russo Ermolli, E., 2012. Evolution of the Sele River coastal plain (southern Italy) during the Late Quaternary by inland and offshore stratigraphical analyses. Rendiconti Lincei 23, 81–102.
Barra, D., Calderoni, G., Cinque, A., De Vita, P., Rosskopf, C.M., Russo Ermolli, E., 1998. New data on the evolution of the Sele river coastal plain (southern Italy) during the Holocene. Il Quat. 11, 287–299.
Barra, D., Romano, P., Santo, A., Campajola, L., Roca, V., Tuniz, C., 1996. The Versilian transgression in the Volturno River Plain (Campania, southern Italy): palaeoenvironmental history and chronological data. Il Quat. 9, 445–458.
Belluomini, G., Caldara, M., Casini, C., Cerasoli, M., Manfra, L., Mastronuzzi, G., Palmentola, G., Sanso, P., Tuccimei, P., Vesica, P.L., 2002. The age of Late Pleistocene shorelines and tectonic activity of Taranto area, Southern Italy. Quat. Sci. Rev. 21, 525–547.
Benjamin, J., Rovere, A., Fontana, A., Furlani, S., Vacchi, M., Inglis, R.H., Galili, E., Antonioli, F., Sivan, D., Miko, S., Mourtzas, N., Felja, I., Meredith-Williams, M., Goodman-Tchernov, B., Kolaiti, E., Anzidei, M., Gehrels, R., 2017. Late Quaternary sea-level changes and early human societies in the central and eastern Mediterranean Basin: an interdisciplinary review. Quat. Int. 449, 29–57.
Brückner, H., 1980. Marine terrassen in Süditalien. Eine quartärmorphologische Studie über das Kustentiefland von Metapont.
Caputo, R., Bianca, M., D'Onofrio, R., 2010. Ionian marine terraces of southern Italy: insights into the Quaternary tectonic evolution of the area. Tectonics 29, TC4005,. https://doi.org/10.1029/2009TC002625.
Carobene, L., 2003. Genesis, age, uplift and erosion of the marine terraces of Crosia-Calopezzati (Ionian coast of Calabria, Italy). Il Quat. 16, 43–90.
Ciaranfi, N., Ghisetti, F., Guida, M., Iaccarino, G., Lambiase, S., Pieri, P., Rapisardi, L., Ricchetti, G., Torre, M., Tortorici, L., Vezzani, L., 1983. Carta Neotettonica dell'Italia Meridionale, Prog. Fin. Geod, vol. 515. CNR, Rome, p. 62.
Cilumbriello, A., Sabato, L., Tropeano, M., Gallicchio, S., Grippa, A., Maiorano, P., Mateu-Vicens, G., Rossi, C.A., Spilotro, G., Calcagnile, L., Quarta, G., 2010. Sedimentology, stratigraphic architecture and preliminary hydrostratigraphy of the Metaponto coastal-plain subsurface (Southern Italy). Memorie Descrittive Carta Geologica d'Italia 90, 67–84.
Cocco, E., De Pippo, T., Pennetta, M., 1976. L'uso della fotografia aerea e del calcolatore elettronico nello studio degli spostamenti delle linee di costa: l'evoluzione del litorale Alto Ionico (Golfo di Taranto) negli ultimi 30 anni. Boll. Soc. Geol. Ital. 95, 275–312.
Corrado, G., Amodio, S., Aucelli, P.P.C., Incontri, P., Pappone, G., Schiattarella, M., 2018. Late Quaternary geology and morphoevolution of the Volturno coastal plain, southern Italy. Alpine and Mediterranean Quaternary 31, 23–26.
Corrado, G., Amodio, S., Aucelli, P.P.C., Pappone, G., Schiattarella, M., 2020. The subsurface geology and landscape evolution of the Volturno coastal plain, Italy: interplay between tectonics and sea-level changes during the quaternary. Water 12, 3386.
Corrado, G., Di Leo, P., Giannandrea, P., Schiattarella, M., 2017. Constraints on the dispersal of Mt. Vulture pyroclastic products: implications to mid- Pleistocene climate conditions in the foredeep domain of southern Italy. Geomorphologie: relief, Processus. Environment 23, 171–182.
Cucci, L., Cinti, F.R., 1998. Regional uplift and local tectonic deformation recorded by the Quaternary marine terraces on the Ionian coast of northern Calabria (southern Italy). Tectonophysics 292, 67–83.
Dai Pra, G., Hearty, P.J., 1988. I livelli marini pleistocenici del Golfo di Taranto. Sintesi Geocronostratigrafica e tettonica. Mem. Soc. Geol. Ital.c 41, 637–644.
De Santis, V., Caldara, M., Torres, T., Ortiz, J.E., Sánchez-Palencia, Y., 2018. A review of MIS 7 and MIS 5 terrace deposits along the Gulf of Taranto based on new stratigraphic and chronological data. Ital. J. Geosci. 137, 349–368.
Di Lorenzo, H., Aucelli, P., Corrado, G., De Iorio, M., Schiattarella, M., Russo Ermolli, E., 2021. Environmental evolution and anthropogenic forcing in the Garigliano coastal plain (Italy) during the Holocene. Holocene 31 (7), 1089–1099.
Di Paola, G., Alberico, I., Aucelli, P.P.C., Matano, F., Rizzo, A., Vilardo, G., 2018. Coastal subsidence detected by Synthetic Aperture Radar interferometry and its effects coupled with future sea-level rise: the case of the Sele Plain (Southern Italy). J. Flood Risk Manag. 11, 191–206.
Doglioni, C., Mongelli, F., Pieri, P., 1994. The Puglia uplift (SE-Italy): an anomaly in the foreland of the Apenninic subduction due to buckling of a thick continental litosphere. Tectonics 13, 1309–1321.
Doglioni, C., Tropeano, M., Mongelli, F., Pieri, P., 1996. Middle-late Pleistocene uplift of Puglia: an "anomaly" in the apenninic foreland. Mem. Soc. Geol. Ital. 51, 101–117.
Fagerstrom, J.A., 1964. Fossil communities in Paleoecology: their recognition and significance. GSA Bulletin 75, 1197–1216.
Ferranti, L., Pagliarulo, R., Antonioli, F., Randisi, A., 2011. "Punishment for the Sinner": Holocene episodic subsidence and steady tectonic motion at ancient Sybaris (Calabria, southern Italy). Quat. Int. 232, 56–70.
Giardino, L., 1991. Grumentum e Metaponto. Due esempi di passaggio dal tardoantico all'alto medioevo in Basilicata. Mélanges de l'École française de Rome. Le. Moyen Age 103, 827–858.
Gillot, P.Y., Kieffer, G., Romano, R., 1994. Evolution of Mount Etna volcano in the light of potassium-argon dating. Acta Vulcanol. 5, 81–87.
Gioia, D., Bavusi, M., Di Leo, P., Giammatteo, T., Schiattarella, M., 2016. A geoarchaeological study of the Metaponto coastal belt, southern Italy, based on geomorphological mapping and Gis-supported classification of landforms. Geogr. Fis. Din. Quaternaria 39, 137–147.
Gioia, D., Bavusi, M., Di Leo, P., Giammatteo, T., Schiattarella, M., 2020. Geoarchaeology and geomorphology of the Metaponto area, Ionian coastal belt, Italy. J. Maps 16, 117–125.
Gioia, D., Schiattarella, M., Giano, S., 2018. Right-angle pattern of minor fluvial networks from the ionian terraced belt, southern Italy: passive structural control or foreland bending? Geosciences 8, 331.
Grippa, A., Bianca, M., Tropeano, M., Cilumbriello, A., Gallipoli, M.R., Mucciarelli, M., Sabato, L., 2011. Use of the HVSR method to detect buried paleomorphologies (filled incised-valleys) below a coastal plain: the case of the Metaponto plain (Basilicata, southern Italy). Bollettino Di Geofisica Teorica. In: Applicata, vol. 52, pp. 225–240.
Hammer, Ø., Harper, D.A.T., Paul, D.R., 2001. Past: paleontological statistics software package for education and data analysis. Palaeontol. Electron. 4, 1–9.
Lambeck, K., Antonioli, F., Anzidei, M., Ferranti, L., Leoni, G., Scicchitano, G., Silenzi, S., 2011. Sea Level Change Along the Italian Coast During the Holocene and Projections for the Future, 232, pp. 250–257.
Lisiecki, L.E., Raymo, M.E., 2005. Pliocene-Pleistocene stack of globally distributed benthic stable oxygen isotope records, Supplement to: Lisiecki, LE; Raymo, ME: a Pliocene-Pleistocene stack of 57 globally distributed benthic d18O records. Paleoceanography. https://doi.org/10.1029/2004PA001071, 20, PA1003, PANGAEA.
Marturano, A., Aiello, G., Barra, D., 2011. Evidence for late Pleistocene uplift at the Somma-Vesuvius apron near Pompeii. J. Volcanol. Geoth. Res. 202, 211–227.
Matano, F., 2019. Analysis and classification of natural and human-induced ground deformations at regional scale (Campania, Italy) detected by satellite synthetic-aperture radar interferometry archive datasets. Rem. Sens. 11.
Meisch, C., 2000. Freshwater Ostracoda of western and central Europe. In: Spektrum Adademischer Verlag, p. 522. Heidelberg, Germany.
Migliorini, C., 1937. Cenno sullo studio e sulla prospezione petrolifera di una zona dell'Italia meridionale. 2nd Petroleum world Congress, Paris. AGIP report, Roma, pp. 1–11.
Molin, P., Dramis, F., Lupia Palmieri, E., 2002. The Pliocene-quaternaty uplift of the ionian northern Calabria coastal belt between Corigliano Calabro and Capo Trionto. Studi Geologici Camerti Spec 135–145. Vol.
Monaco, C., Tapponnier, P., Tortorici, L., Gillot, P.Y., 1997. Late Quaternary slip rates on the Acireale-Piedimonte normal faults and tectonic origin of Mt. Etna (Sicily). Earth Planet Sci. Lett. 147, 125–139.
Monaco, C., Bianca, M., Catalano, S., De Guidi, G., Tortorici, L., 2002. Sudden change in the Late Quaternary tectonic regime in eastern Sicily: evidences from geological and geomorphological features. Boll. Soc. Geol. Ital. 1, 901–913.
Patterson, R.T., Fishbein, E., 1989. Re-examination of the statistical methods used to determine the number of point counts needed for micropaleontological quantitative research. J. Paleontol. 63 (2), 245–248.
Pescatore, T., Pieri, P., Sabato, L., Senatore, M.R., Gallicchio, S., Boscaino, M., Cilumbriello, A., Quarantiello, R., Capretto, G., 2009. Stratigrafia dei depositi pleistocenico-olocenici dell'area costiera di Metaponto compresa fra Marina di Ginosa. In: Il Torrente Cavone (Italia Meridionale): Carta Geologica in Scala 1: 25.000. Il Quaternario, vol. 22, pp. 307–324.
Piccarreta, M., Caldara, M., Capolongo, D., Boenzi, F., 2011. Holocene geomorphic activity related to climatic change and human impact in Basilicata, Southern Italy. Geomorphology 128, 137–147.
Polcari, M., Albano, M., Montuori, A., Bignami, C., Tolomei, C., Pezzo, G., Falcone, S., La Piana, C., Doumaz, F., Salvi, S., Stramondo, S., 2018. InSAR monitoring of Italian coastline revealing natural and anthropogenic ground deformation phenomena and future perspectives. Sustainability 10.

Reimer, P.J., Bard, E., Bayliss, A., Beck, J.W., Blackwell, P.G., Ramsey, C.B., Buck, C.E., Cheng, H., Edwards, R.L., Friedrich, M., Grootes, P.M., Guilderson, T.P., Haflidason, H., Hajdas, I., Hatté, C., Heaton, T.J., Hoffmann, D.L., Hogg, A.G., Hughen, K.A., Kaiser, K.F., Kromer, B., Manning, S.W., Niu, M., Reimer, R.W., Richards, D.A., Scott, E.M., Southon, J.R., Staff, R.A., Turney, C.S.M., van der Plicht, J., 2016. IntCal13 and Marine13 radiocarbon age calibration curves 0–50,000 Years cal BP. Radiocarbon 55, 1869–1887.

Robustelli, G., Lucà, F., Corbi, F., Pelle, T., Dramis, F., Fubelli, G., Scarciglia, F., Muto, F., Cugliari, D., 2009. Alluvial terraces on the Ionian coast of northern Calabria, southern Italy: implications for tectonic and sea level controls. Geomorphology 106, 165–179.

Sabato, L., Longhitano, S.G., Gioia, D., Cilumbriello, A., Spalluto, L., 2012. Sedimentological and morpho-evolution maps of the 'Bosco Pantano di Policoro' coastal system (Gulf of Taranto, southern Italy). J. Maps 8, 304–311.

Santoro, E., Ferranti, L., Burrato, P., Mazzella, M.E., Monaco, C., 2013. Deformed Pleistocene marine terraces along the Ionian Sea margin of southern Italy: unveiling blind fault-related folds contribution to coastal uplift. Tectonics 32, 737–762.

Sauer, D., Wagner, S., Bruckner, H., Scarciglia, F., Mastronuzzi, G., Stahr, K., 2010. Soil development on marine terraces near Metaponto (Gulf of Taranto, southern Italy). Quat. Int. 222, 48–63.

Schaeffer, M., Hare, W., Rahmstorf, S., Vermeer, M., 2012. Long-term sea-level rise implied by 1.5 °C and 2 °C warming levels. Nat. Clim. Change 2, 867–870.

Schiattarella, M., Leo, P.D., Beneduce, P., Giano, S.I., Martino, C., 2006. Tectonically driven exhumation of a young orogen: an example from the southern Apennines, Italy. In: Willett, S.D., Hovius, N., Brandon, M.T., Fisher, D. (Eds.), Geol S Am S. Special Paper of the Geological Society of America, vol. 398, pp. 371–385.

Sgarrella, F., Barra, D., 1985. Distribuzione dei Foraminiferi bentonici nel Golfo di Salerno (Basso Tirreno, Italia). Bollettino della Soc. dei Nat. Napoli 93, 1–58.

Shackleton, N.J., 1987. Oxygen isotopes, ice volume and sea level. Quat. Sci. Rev. 6, 183–190.

Tropeano, M., Cilumbriello, A., Sabato, L., Gallicchio, S., Grippa, A., Longhitano, S.G., Bianca, M., Gallipoli, M.R., Mucciarelli, M., Spilotro, G., 2013. Surface and subsurface of the Metaponto coastal plain (Gulf of Taranto-southern Italy): present-day- vs LGM-landscape. Geomorphology 203, 115–131.

Tropeano, M., Sabato, L., Pieri, P., 2002. Filling and cannibalization of a foredeep: the Bradanic trough, southern Italy. Sediment flux to basins: causes. Control and Consequences 191, 55–79.

Westaway, R., 1993. Quaternary uplift of southern Italy. J. Geophys. Res. Solid Earth 98, 21741–21772.

Westaway, R., Bridgland, D., 2007. Late Cenozoic uplift of southern Italy deduced from fluvial and marine sediments: coupling between surface processes and lower-crustal flow. Quat. Int. 175, 86–124.

Wöppelmann, G., Marcos, M., 2016. Vertical land motion as a key to understanding sea level change and variability. Rev. Geophys. 54, 64–92.

Zander, A., Fulling, A., Bruckner, H., Mastronuzzi, G., 2006. OSL dating of Upper Pleistocene littoral sediments: a contribution to the chronostratigraphy of raised marine terraces bordering the Gulf of Taranto, South Italy. Geogr. Fis. Din. Quaternaria 29, 33–50.

Zuschin, M., Stachowitsch, M., Stanton, R.J., 2003. Patterns and processes of shell fragmentation in modern and ancient marine environments. Earth Sci. Rev. 63, 33–82.